KPZ GROWTH DURING SURFACE RECONSTRUCTION AND AS AN AVALANCHE PROCESS

Chen-Shan Chin
Chun-Chung Chen
and
Marcel den Nijs

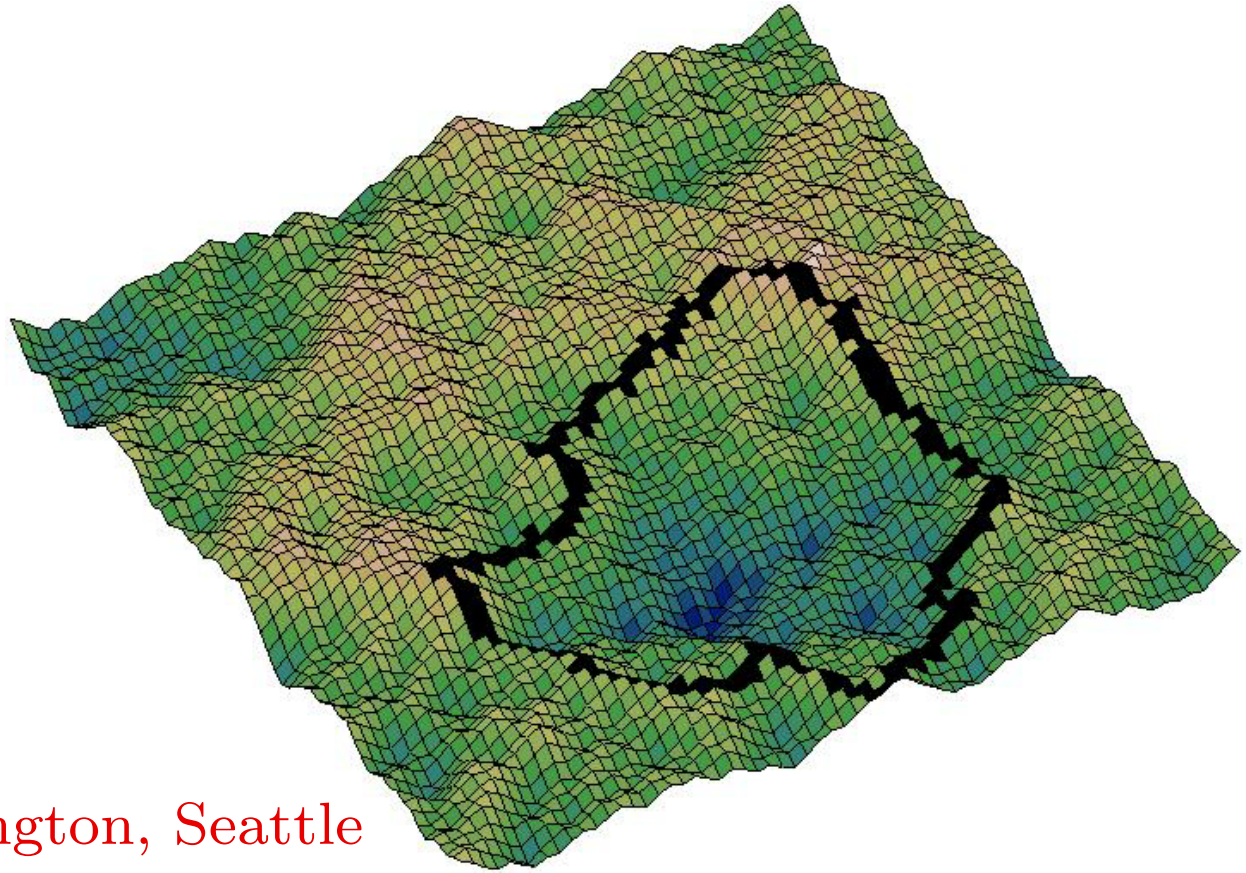

University of Washington, Seattle

supported by NSF grant DMR-9985806

OUTLINE:

A: Introduction to KPZ growth

B: Stationary State Skewness and finite size scaling corrections in 2D KPZ Growth

CSC and MdN, PRE 59, 2633 (1999)

C: Reconstructed Rough Growing Interfaces, Ridge Line Trapping of Domain Walls,

CSC and MdN, PRE 64, 031606 (2001)

D: An Interface View of Directed Sandpile Dynamics

CCC and MdN, PRE 65, March (2002), in press

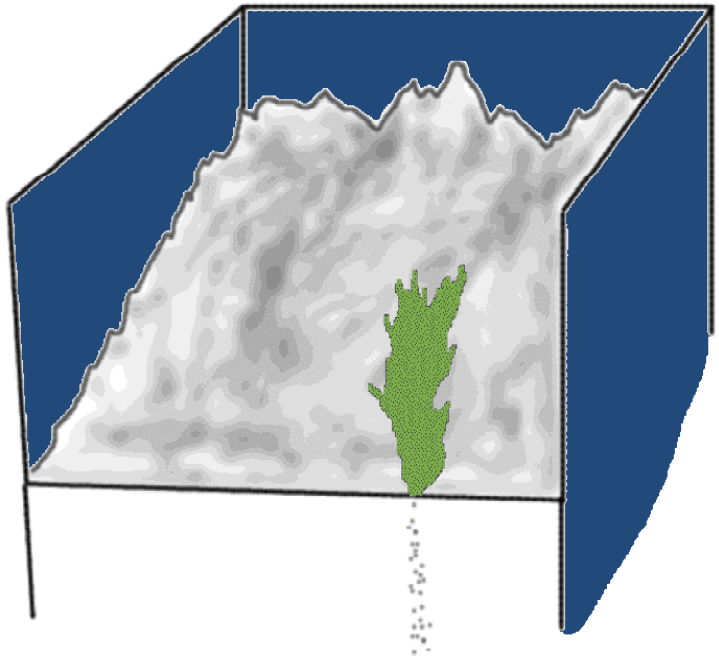

A. INTRODUCTION TO KPZ SURFACE GROWTH

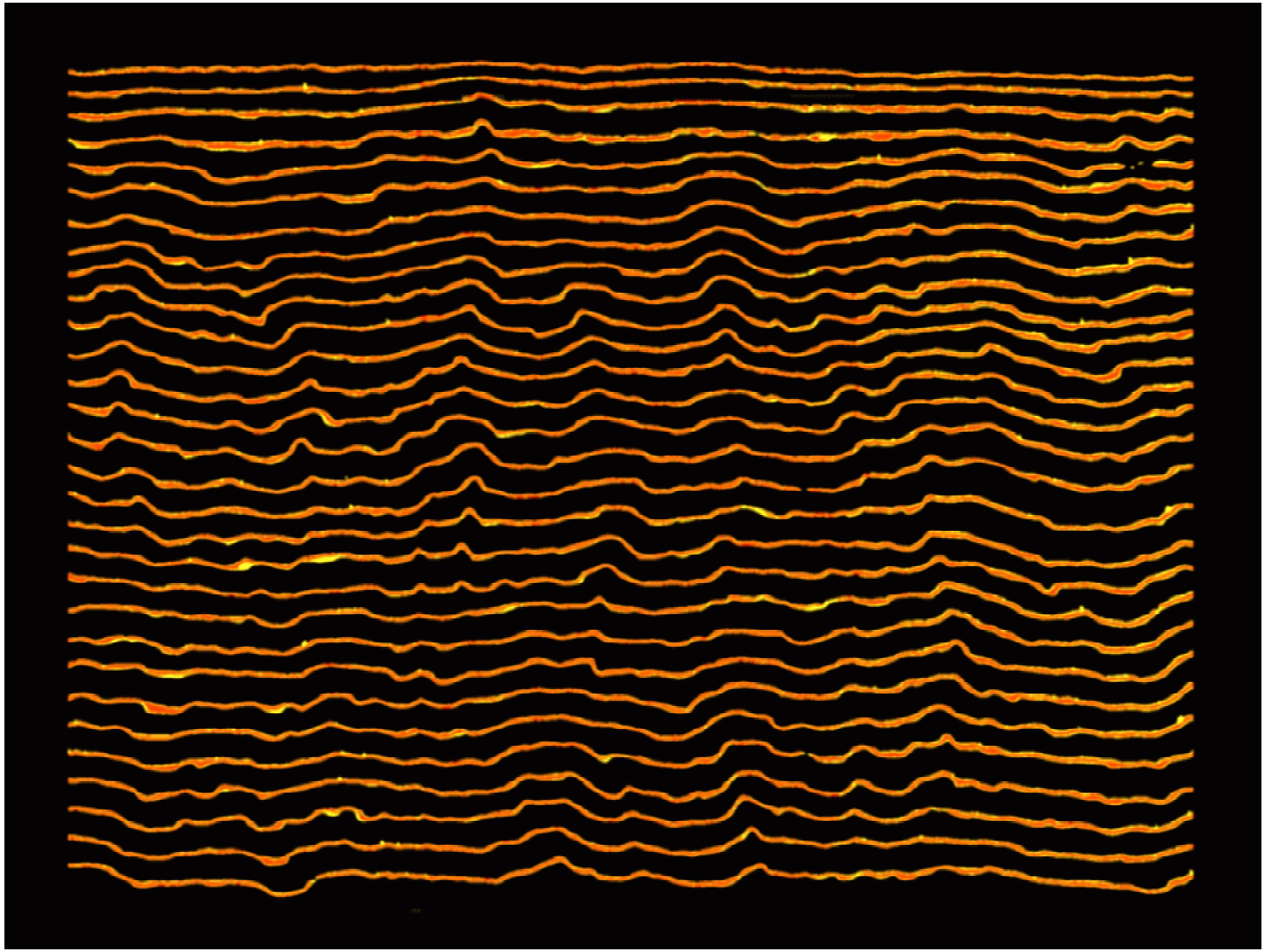

1. The KPZ Langevin equation

$$\frac{d}{dt}h(\vec{r},t) = v_0 + \nu\nabla^2 h + \frac{1}{2}\lambda(\nabla h)^2 + \eta$$

with uncorrelated Gaussian noise

$$\langle \eta_{r_2,t_2}\eta_{r_1,t_1}\rangle = 2\Gamma\delta_{r_1,r_2}\delta_{t_1 t_2}$$

Introduced by Kardar, Parisi, and Zhang in 1986.

The bare growth rate v_0 is modified by the local curvature of the surface (the ν-term), its local slope (the λ-term), and random fluctuations (the η-term).

2. The Burgers equation

For randomly stirred vortex (curl) free fluids is equivalent to the KPZ equation (at $\lambda \equiv 1$).

$$\frac{d\vec{v}}{dt} + \lambda \vec{v} \cdot \vec{\nabla} \vec{v} = \nu \nabla^2 \vec{v} + \vec{f}(\vec{r}, t)$$

with velocity $\vec{v}(r) = -\vec{\nabla} h(r)$, viscosity ν, and random force $\vec{f} = -\vec{\nabla} \eta$.

The non-linear λ term arises here logically as part of the total derivative of the velocity.

This formulation is much older than KPZ; e.g., the momentum space ϵ-expansion type RT was worked out in the mid 70-ties by Forster, Nelson, and Stephen.

3. Edwards-Wilkenson (EW) growth

The non-linear λ term is the soul of the KPZ equation.

In it absence the equation becomes linear and reduces to stochastic diffusion, which is trivially soluble,

$$\frac{dh}{dt} = v_0 + \nu\nabla^2 h + \eta.$$

Studies of surface growth by linear equations like this date back to at least the 1950-ties, e.g, Mullins work.

In some growth models λ can be tuned-off accidentally, but in general the non-linear KPZ term is present.

The EW fixed point is unstable under renormalization with respect to (only) the λ term.

4. Thermal equilibrium

The EW equation describes how a surface reaches thermal equilibrium in the absence of a driving force; λ and v_0 are typically both proportional to the growth rate.

At high temperatures the equilibrium surface is rough, and its energy is described by the Gaussian form

$$E(\{h(r)\}) = \int dh \, \frac{1}{2}\nu(\nabla h)^2.$$

Monte Carlo simulations, and other elementary dynamic processes lead typically to the detailed balance Langevin equation

$$\frac{\partial h}{\partial t} = -\frac{\delta E}{\delta h} + \eta \rightarrow \text{ EW equation.}$$

5. EW scale invariance

Renormalization transformations reduce to so-called power counting for linear processes. The EW equation

$$\frac{dh}{dt} = v_0 + \nu\nabla^2 h + \eta, \quad \langle \eta_{r_2,t_2}\eta_{r_1,t_1}\rangle = 2\Gamma\delta_{r_1,r_2}\delta_{t_1 t_2}$$

is term-by-term invariant under rescaling: $h' = b^{-\alpha}h$, $t' = b^{-z}t$, $r' = b^{-1}r$, $\nu' = b^{y_\nu}\nu$, $\eta\prime = b^{y_\eta}\eta$, and $\Gamma' = b^{y_\Gamma}\Gamma$, when the scaling exponents have the values:

$$z = 2, \quad \alpha = \frac{1}{2}(2 - D), \quad y_\lambda = 1 - \frac{D}{2}$$

(D= spatial dimension); while by choice $y_\nu = y_\Gamma \equiv 0$.

6. EW Surface Roughness

The moments of the height distribution

$$W_n(L,t) = L^{-1} \sum_r \langle (h_r - h_{av})^n \rangle$$

scale as

$$W_n(t, L, \nu, \lambda) = b^{n\alpha} W_n(b^{-z}t, b^{-1}L, \nu, b^{y_\lambda}\lambda)$$

The surface width diverges in time as $\mathcal{W} = \sqrt{W_2} \sim t^\beta$, with $\beta = \frac{\alpha}{z} = \frac{1}{4}$; and in the stationary state with system size as $\mathcal{W} \sim L^{\frac{1}{2}}$ in 1D, and as $\mathcal{W} \sim \log(L)$ in 2D.

7. KPZ surface roughness

This requires a full scale renormalization transformation, but except for 1D, the strong coupling "KPZ fixed point" remains unkown.

The surface reaches a stationary growing rough state, and the height distribution moments scale as

$$W_n(t, L, \nu, \lambda) = b^{n\alpha} W_n(b^{-z} t, b^{-1} L, b^{\nu}\, \nu, \lambda)$$

Galilean invariance of the Burgers equation implies that

$$y_\lambda = 0 \quad \rightarrow \quad \alpha + z = 2$$

– λ acts as a so-called redundant-marginal scaling field.
– It suffices to study the stationary state.

8. Epsilon-expansion

The one loop ϵ-expansion type renormalization transformation in the parameter $g = \lambda^2 \Gamma / \nu^3$

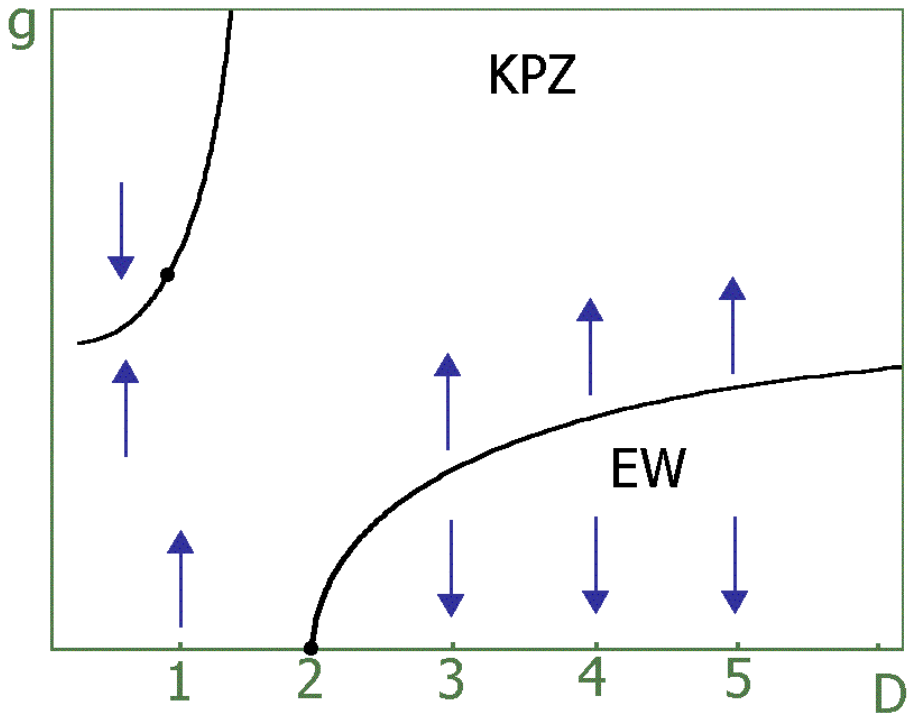

$$\frac{\partial g}{\partial l} = \frac{2-D}{2} g + K \frac{2d-3}{4D} g^3$$

does not yield a KPZ fixed point.

– The EW fixed point at $g = 0$ is unstable for $D < 2$.

– 2 fixed points split-off from EW at $D_c^{EW} = 2$

The 1-th loop correction is of order g^3, instead of, e.g., g^2 in ϕ^4-theory (Ising) where 2 FP's cross at $D_c^{\phi^4} = 4$.

9. RSOS (Kim-Kosterlitz) growth model

– discrete heights lattice version of KPZ growth

– cubic building blocks

– nearest neighbour heights differ by $\Delta h = S_n^z = 0, \pm 1$. (spin-1 type step variables).

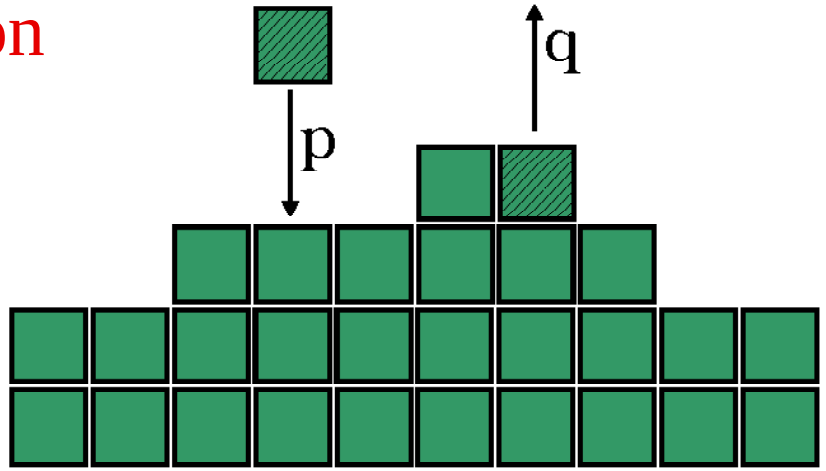

Growth rule: Select at random one of the columns. Attempt an absorption or desorption event. Absorb (disorb) a particle with probability p (q) if the $\Delta h = 0, \pm 1$ constraints remain satisfied.

– sloped areas are less active $\rightarrow \lambda < 0$

– the stationary state is skewed even in 1D.

10. <u>BCSOS (brick laying) growth</u>

- Rectangular building blocks (brick wall on its side).

– Nearest neighbour heights differ by only $\Delta h = S_n^z = \pm 1$.

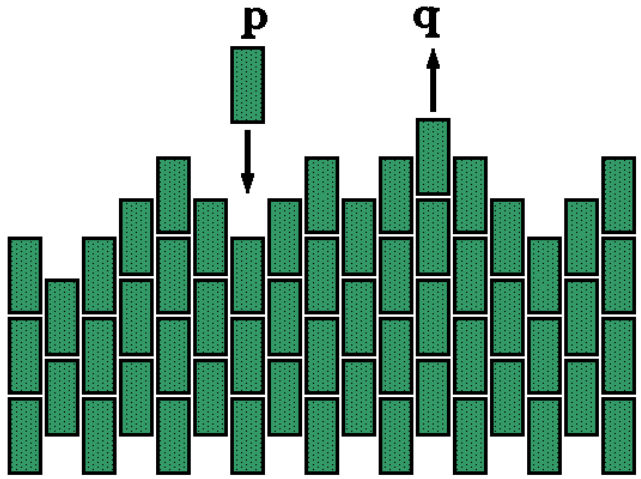

<u>Growth rule:</u> Select at random one of the columns. If this column is the bottom (top) of a local valley (hill top), a particle adsorbs (disorbs) with probability p (q) Local slopes are inactive ($\rightarrow \lambda < 0$).

– Early numerical studies: Meakin, Family, $\cdots$.

– In 1D, surface fully characterized by spin-$\frac{1}{2}$ type step variables $\rightarrow$ Master equation: XXZ quantum spin chain.

– Bethe Ansatz exact solution in 1D: Dhar, Gwa/Spohn.

11. 1+1 dimensional KPZ growth exact results

- The 1D KPZ equation stationary state is exactly known; still the EW Gaussian distribution $\rightarrow \alpha = \frac{1}{2} \rightarrow z = \frac{3}{2}$
- The BCSOS brick growth model has a trivial stationary state: the up/down steps are placed at random.
- BCSOS growth, is exactly soluble by the Bethe Ansatz $\rightarrow z = \frac{3}{2}$ (for Galilean invariance skeptics).
- The EW fixed point is unstable with relevant crossover exponent $y_\lambda = \frac{1}{2}$. EW crossover scaling yields $z = z_{EW} - y_\lambda = 2 - \frac{1}{2} = \frac{3}{2}$, with as only presumption that λ is a redundant scaling field for KPZ.

12. Master equation of the BCSOS model

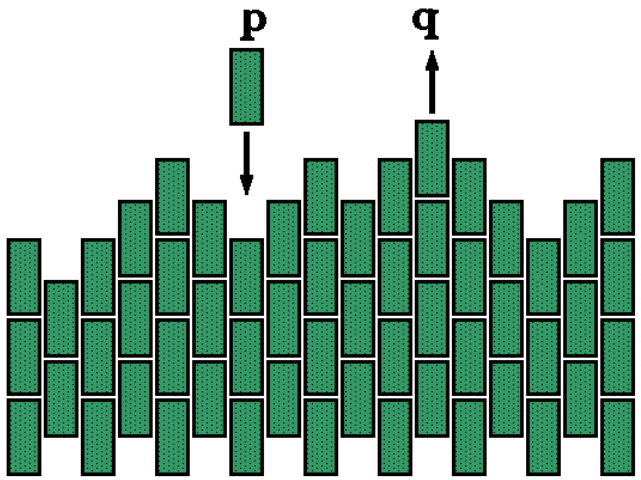

$$|\Psi\rangle_{t+1} = \hat{\mathcal{T}}|\Psi\rangle_t$$

evolves probability distribution

$$|\Psi\rangle = \sum_{\{S_n^z\}} P(\{S_n^z\})\,|\{S_n^z\}\rangle.$$

with time evolution operator

$$\hat{\mathcal{T}} = \frac{1}{N}\sum_n \hat{\mathcal{T}}_{n,n+1}.$$

$$\hat{\mathcal{T}}_{n,n+1} = \left[(1-p) + p\hat{S}_n^+\hat{S}_{n+1}^-\right]\delta(\downarrow\uparrow)_{n,n+1}$$
$$+ \left[(1-q) + q\hat{S}_n^-\hat{S}_{n+1}^+\right]\delta(\uparrow\downarrow)_{n,n+1}$$
$$+ \delta(\downarrow\downarrow)_{n,n+1} + \delta(\uparrow\uparrow)_{n,n+1}$$

13. BCSOS growth and XXZ quantum spin-$\frac{1}{2}$ chains

The time evolution operator, $\hat{\mathcal{T}} = 1 - \frac{1}{N}\sum_n \hat{\mathcal{H}}_{n,n+1}$ is a non-hermitian XXZ spin-$\frac{1}{2}$ Hamiltonian

$$\hat{\mathcal{H}}_{n,n+1} = \frac{1}{4}\epsilon\Big[1 - \mu\hat{S}^z_n\hat{S}^z_{n+1} - 2(\hat{S}^+_n\hat{S}^-_{n+1} + \hat{S}^-_n\hat{S}^+_{n+1}) - 2s(\hat{S}^+_n\hat{S}^-_{n+1} - \hat{S}^-_n\hat{S}^+_{n+1})\Big]$$

with $\mu = 1$, $s = \frac{p-q}{p+q}$, and $\epsilon = p + q$; and
$\delta(\uparrow) = \frac{1}{2}(1 + S^z)$ and $\delta(\downarrow) = \frac{1}{2}(1 - S^z)$.

The master equation of the 1D BCSOS model is a rather special line in the XXZ model, where $\hat{H}$ is stochastic.

14. Experimental realizations: crystal growth (?)

KPZ growth plays a similar role in surface growth as the Ising model in equilibrium critical phenomena.

How do not-included aspects change the universality class: surface diffusion, conservation of particles during epitaxial growth, coupling with other degrees of freedom (like heat diffusion), $\cdots$?

Some aspects are known to be irrelevant, but only at very large length/times scales, much larger than typical experimental ones. Example: layer-by-layer growth (step flow) takes place at temperatures below the equilibrium roughening T and small driving force; the surface looks flat and is only asymptotically rough.

15. Experimental realizations: slow combustion of paper

Slow flameless type combustion of paper is one of few experimentally confirmed KPZ processes
(Jussi Timonen's group in Jyvaskyla, Finland).

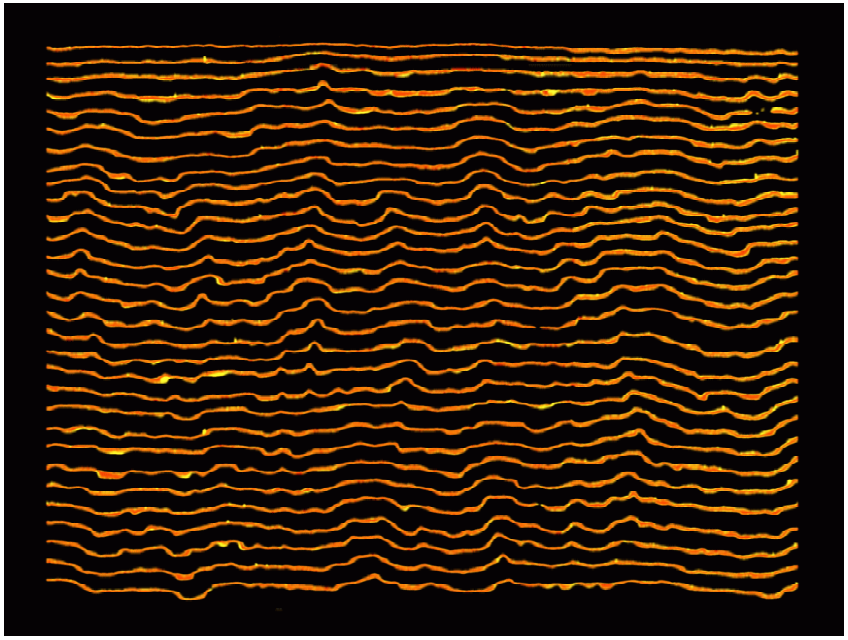

After many sheets of copier and lens paper going up in smoke and ash (it is slow flameless type combustion) they obtain accurate statistical data for the interface width exponents.

15.b. Flameless paper combustion (cont.)

At length scales larger than $r_c \simeq 0.5$ cm the exponents agree with 1D KPZ scaling: $\beta = z/\alpha \simeq 0.35(1)$ and $\alpha \simeq 0.49(2)$.

Below r_c the front is rougher (visible as local bumps in the fronts). The current discussion centers on whether this crossover is due to directed percolation type depinning.

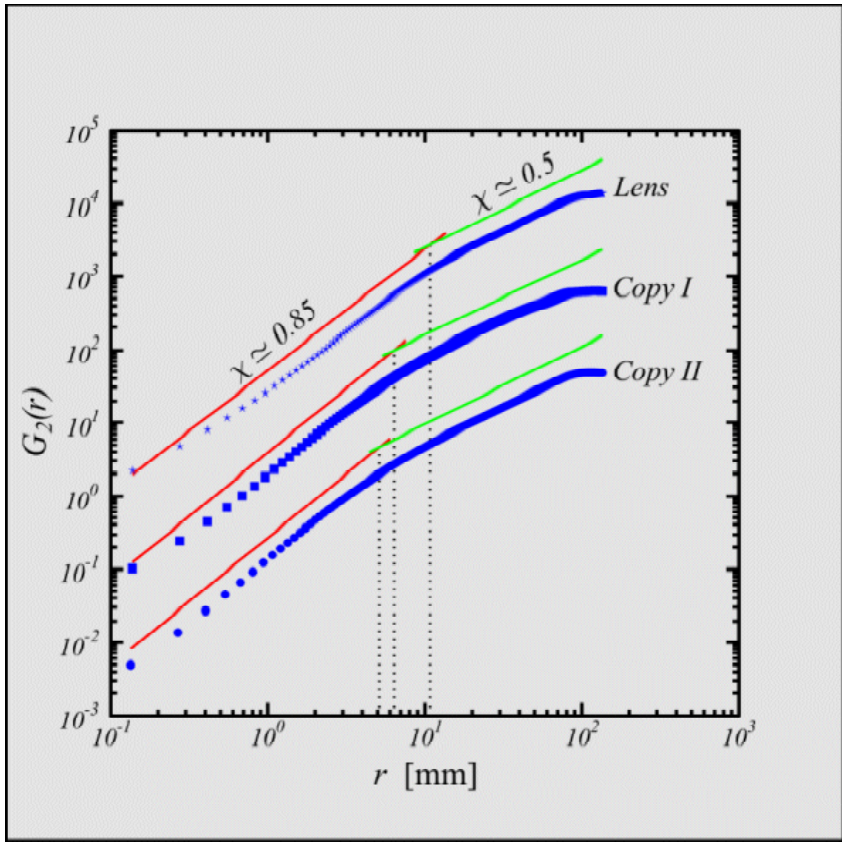

16. Reincarnations: Asymmetric Exclusion Process

The BCSOS model (KPZ growth) represents a driven flow of particles with hard core repulsive interactions:

a Burgers equation on a lattice with discrete velocities.

Interpret the $S_n^z = +1$ up-steps as particles and the $S_n^z = -1$ down-steps as empty sites on the road.

The stationary flowing state is disordered, random, without any correlations, but fluctuations scale in time as $l \sim t^{1/z}$ with the KPZ dynamic exponent $z = \frac{3}{2}$.

Phase transitions take place in open road set-ups with reservoirs on both ends (e.g., Derrida $et.al.$) and when closed by a parking garage (Meesoon Ha and MdN).

17. Reincarnations: Polymer in a random medium

The Hopf transformation maps the KPZ equation onto an Euclidean time Schrödinger (diffusion) equation

$$W(r,t) = e^{\frac{\lambda}{2\nu}h(r,t)} \rightarrow \frac{dW}{dt} = K\nabla^2 W - \eta W.$$

This describes a single particle (a random walker) subject to a quenched random potential that varies both in time and space.

The path integral yields the equilibrium configurations of a directed polymer in a random potential.

This random walker spreads in time as $x \sim t^{1/z}$ with $z = z_{kpz} = \frac{3}{2}$ instead of $z = 2$, the free RW value.

18. Reincarnations: Equilibrium crystal surfaces

KPZ dynamics, in its BCSOS brick model realization, represents a special line in the phase diagram of the XXZ spin chain where its time evolution is stochastic.

The 1+1D XXZ model is equivalent to the transfer matrix of the 2D equilibrium BCSOS crystal surface model.

1+1D KPZ $\leftrightarrow$ facet ridge endpoints in 2D equilibrium

(but with hairiness (Douglas Davidson and MdN 1999)

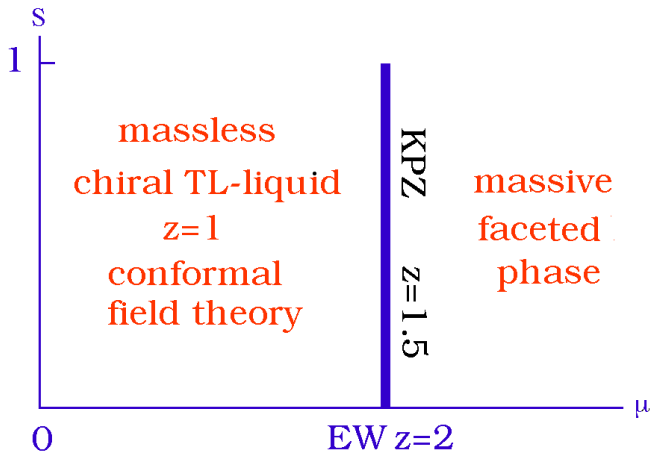

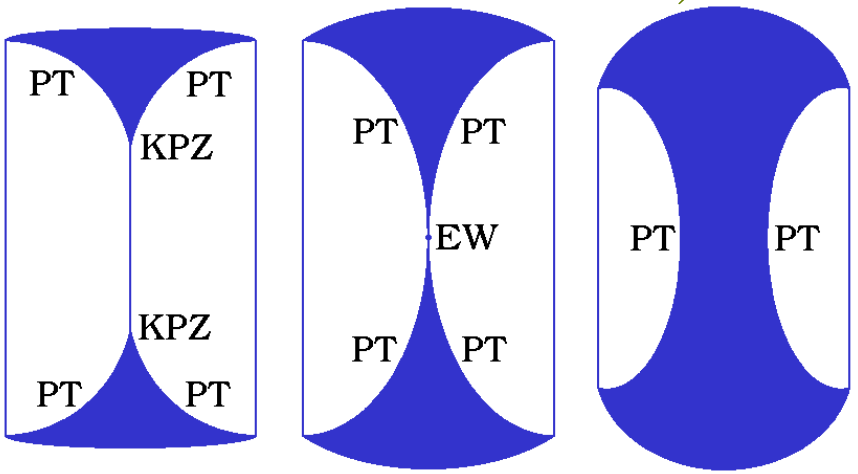

19. KPZ growth in D>1

– The ϵ-expansion type RT with respect to the EW equation does not yield a KPZ fixed point.

– There is no known mean-field theory nor upper critical dimension for KPZ (but lots of discussions about it).

– Many numerical studies, but rarely properly analyzed.

– Michael Lässig's conjecture:

$$\alpha = \frac{2}{n+2} \quad \rightarrow \quad \alpha = \frac{2}{5}, \frac{2}{7}, \cdots$$

Based on the assumption that the operator product expansion of the KPZ correlation functions closes at a specific level of $(\partial^m h / \partial x^m)$. Agrees with an earlier Kim-Kosterlitz conjecture based on numerical data.

B. FINITE SIZE CORRECTIONS TO SCALING AND STATIONARY STATE SKEWNESS IN 2D KPZ GROWTH

Chen-Shan Chin and MdN, PRE 59, 2633 (1999)

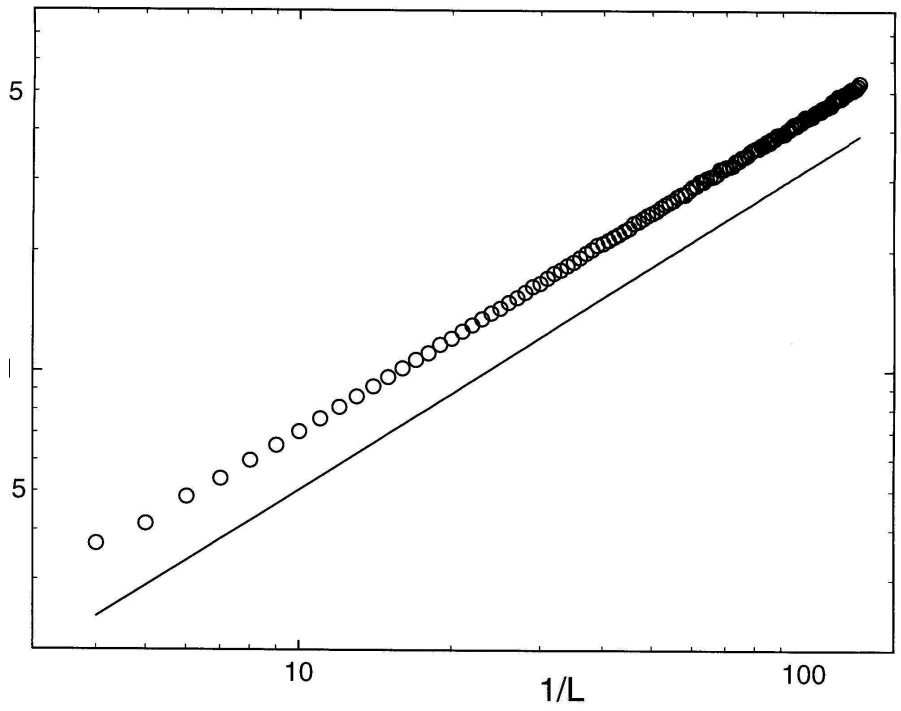

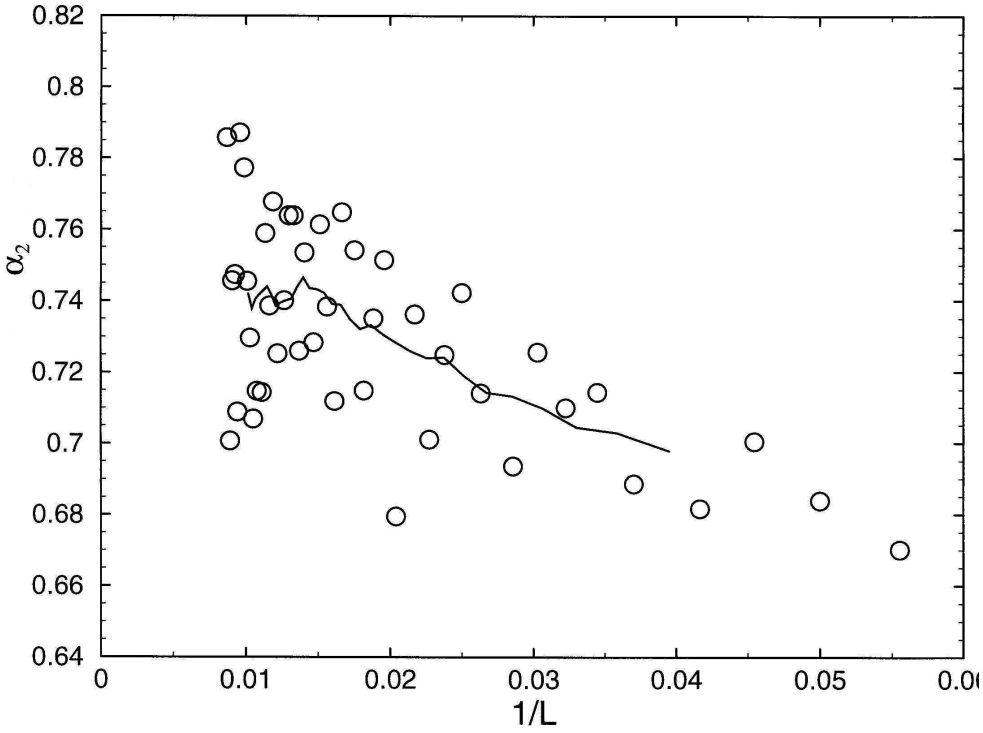

1. Early numerical results for 2D dynamic roughness

Until recently, most numerical studies pretended to be very accurate, with very small quoted error bars, but the values of α between models were mutually inconsistent.

For the 2D BCSOS model, they were in the $\alpha \simeq 0.38$ range while for the 2D Kim-Kosterlitz model $\alpha \simeq 0.40$.

Indifference to this inconsistency illustrates how much universality is taken for granted nowadays.

Such a spread would have been a dead blow for the development of scaling theory during the 1960/70-ties in the context of equilibrium critical phenomena.

How universal are the KPZ exponents in $D > 1$?

2. Corrections to scaling

"Thou shall NEVER deduce the values of critical exponents from straight line fits to log-log plots."

Simple power laws without corrections to scaling are rare.

$W_2 \sim N^{2\alpha}(A + BN^{y_{ir}} + \cdots)$

with $y_{ir} < 0$ is the norm.

Plot the local slopes of the log-log plot as function of N.

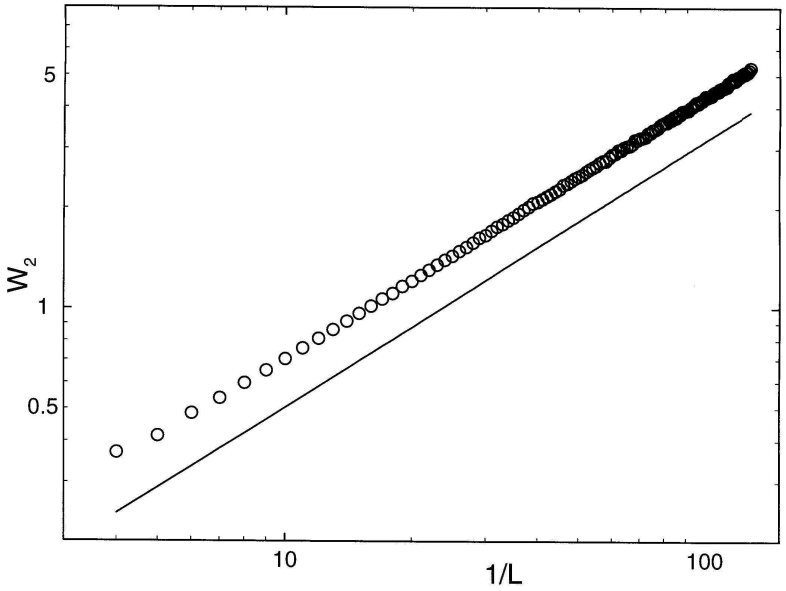

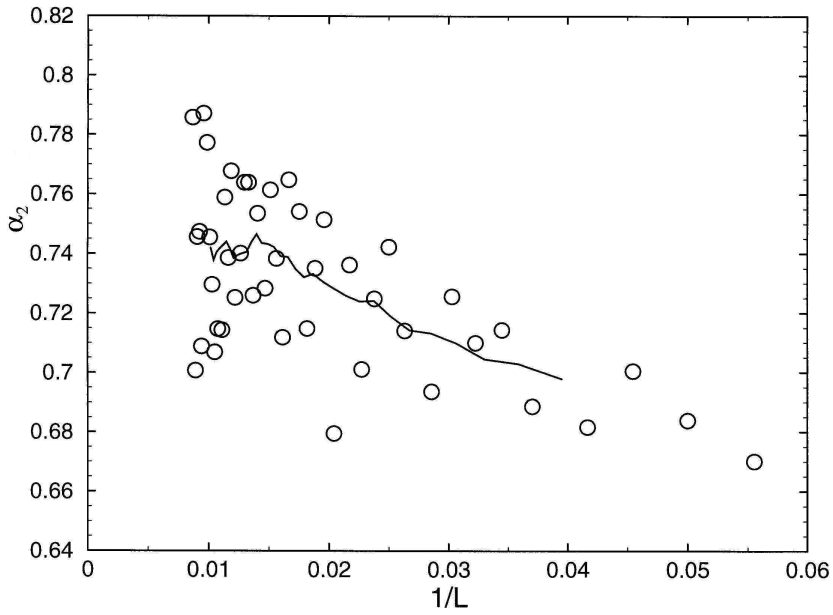

3. Corrections to scaling exponent for the 2-nd moment

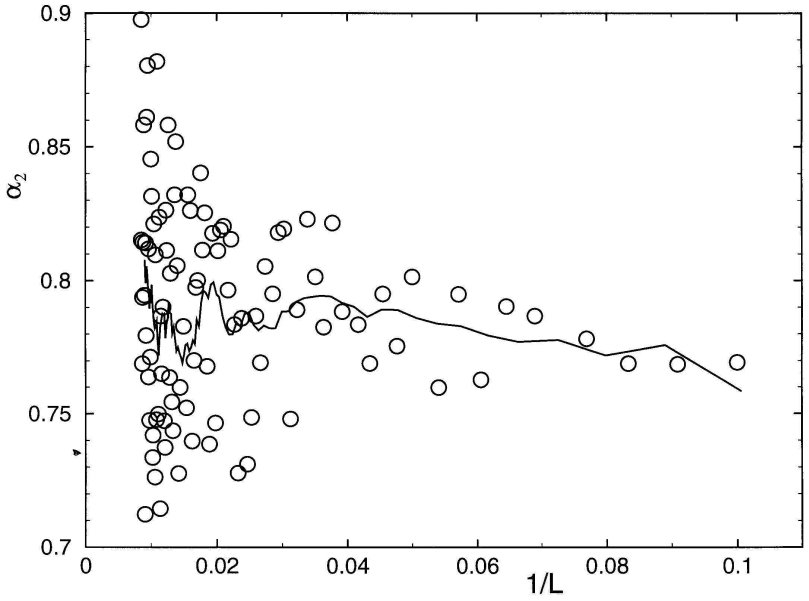

RSOS ↑

BCSOS →

The corrections to scaling are small in RSOS but large in BCSOS growth (further from the fixed point).

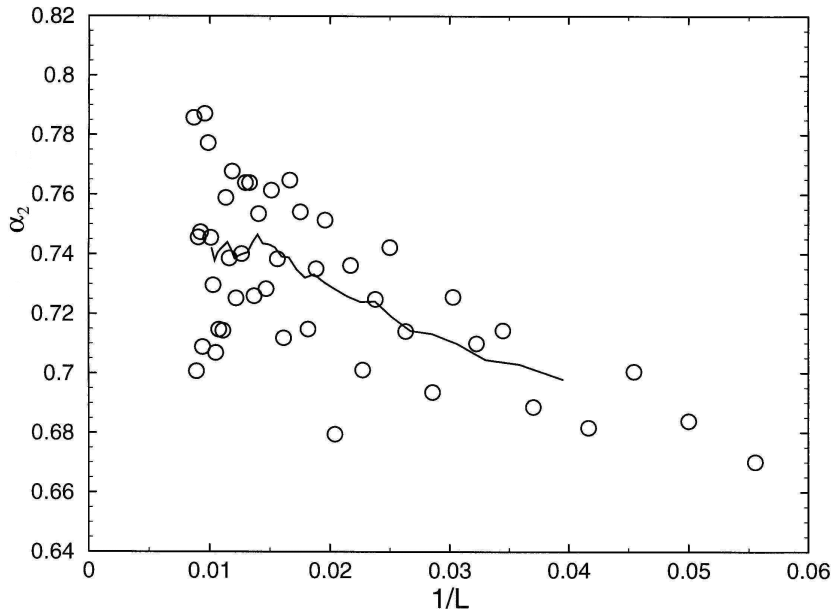

According to Lässig the 2-nd moment scales as

$\alpha_2 = 2 \times \alpha = 0.80$

This requires $y_{ir} = -0.6$ (2)

4. Corrections to scaling exponent for the third moment

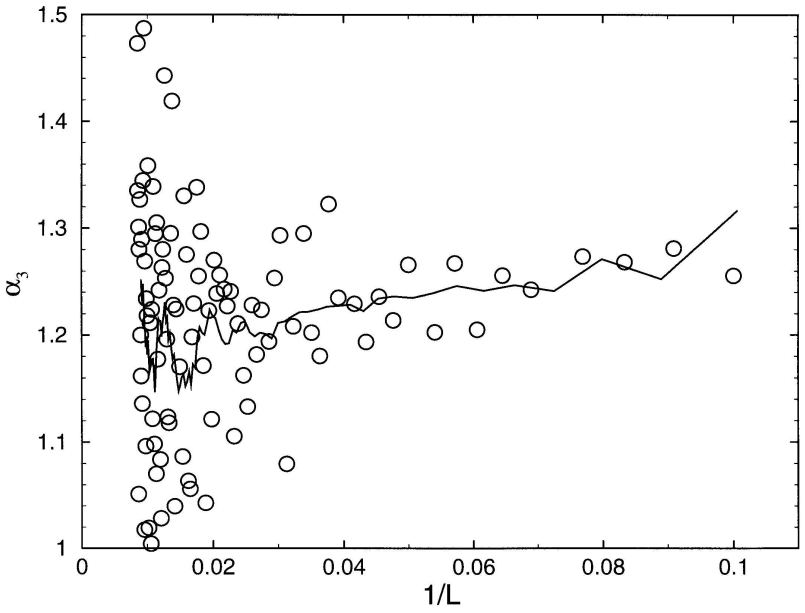

The leading corrections to scaling exponents for the odd and the even moments are different.

RSOS ↑ BCSOS →

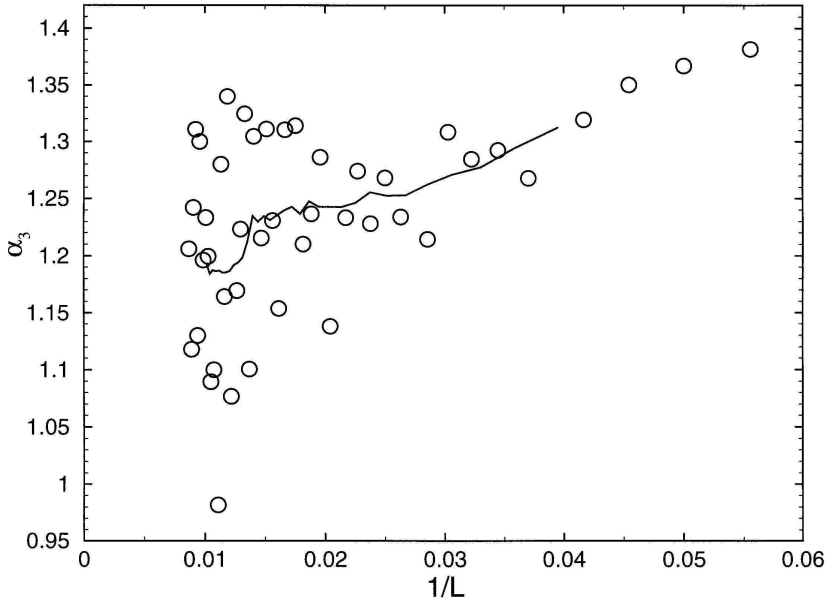

According to Lässig the 3-rd moment scales as

$\alpha_3 = 3 \times \alpha = 1.20$

This requires: $y_{ir} = -1.7$ (3)

5. Corrections to scaling exponent for the fourth moment

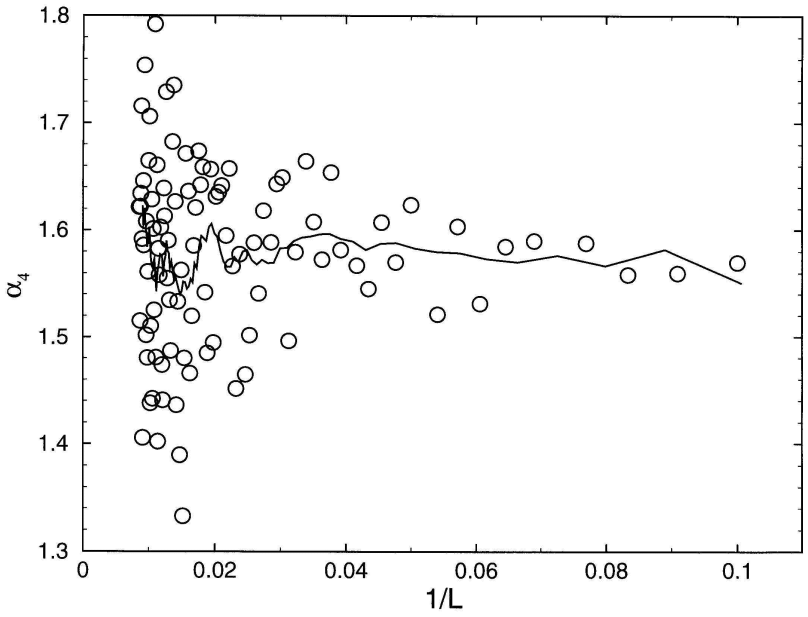

The even moments have the same leading corrections to scaling exponent

RSOS ↑ BCSOS →

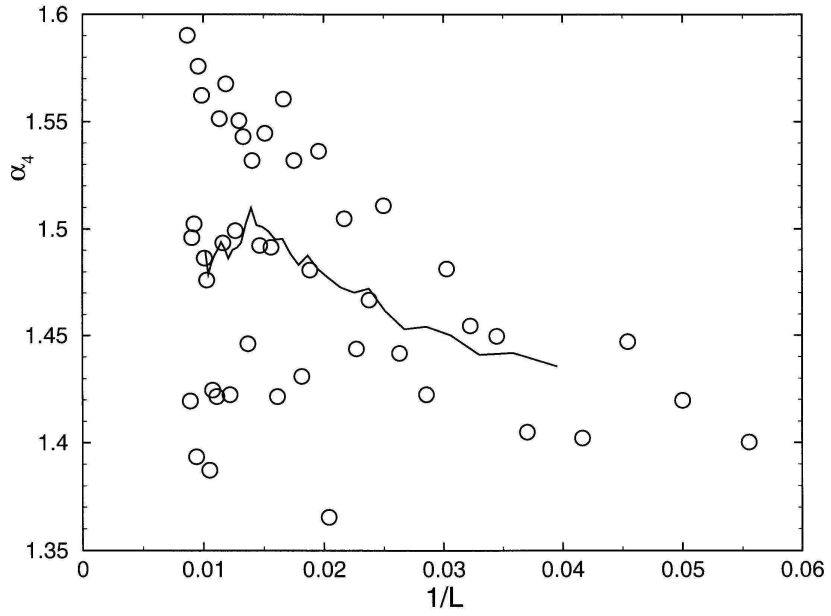

According to Lässig the 4-th moment scales as

$\alpha_4 = 4 \times \alpha = 1.60$

This requires: $y_{ir} = -0.6$ (2)

6. Identifying the corrections to scaling operators

Lässig conjecure presumes that the KPZ operator algebra contains only a few independent elements, and that the scaling exponents of the higher-order operators have power counting values.

Our results, y_{ir}= -0.6 (2) (even)) and y_{ir}= -1.7 (3) (odd moments), are close to what we could expect:

The curvature operator $\partial^2 h/\partial x^2$ is irrelevant, but not by much. Power counting suggests $y_\nu = -\alpha$.

$\partial^2 h/\partial x^2$ does not affect odd moments.

A leading candidate for the odd moments corrections to scaling is $(\partial^2 h/\partial x^2)^2$, with $y_{sk} = -2$.

7. Stationary state skewness

In general, KPZ stationary states lacks particle-hole symmetry. The third moment W_3 is nonzero, even in 1D. The Kim-Kosterlitz model is an example.

Stationary state skewness is distinct from temporal skewness. Most initial states develop skewness at intermediate time scales, even if the stationary state is not skewed (e.g., the 1D BCSOS model).

In 1D, the KPZ fixed point lies at zero skewness. Skewness can be present, but is tunable. It originates from terms that break particle-hole symmetry, such as $(\partial^2 h/\partial x^2)^2$. Their coupling constants u_{sk} are tunable.

8. Stationary state skewness is tunable in 1D

Stationary state height distribution moments scale as

$$W_n(N^{-1}, u_{sk}) = b^{n\alpha} W_n(bN^{-1}, b^{y_{sk}} u_{sk})$$

– Even moments behave as $W_n \simeq AN^{n\alpha} + ...$
with universal amplitude ratio's, $R_n = W_n / W_2^{\frac{n}{2}}$.
– Odd moments scale as

$$\begin{aligned} W_n(N^{-1}, u_{sk}) &= N^{n\alpha} \mathcal{F}_n(N^{y_{sk}} u_{sk}) \\ &= N^{n\alpha} \left[\mathcal{F}_n(0) + \mathcal{F}_n'(0) N^{y_{sk}} u_{sk} + ...\right] \\ &\sim u_{sk} N^{n\alpha + y_{sk}} \end{aligned}$$

since for them $\mathcal{F}_n(0) = 0$ at the fixed point. The odd amplitude ratio's are proportional to u_{sk} and thus are not universal. $y_{sk} \simeq -1$ (John Neergaard+MdN).

9. Local versus global skewness

A visualization of skewness is a landscape where on average hill tops are wider (flatter, less sharp) than valley bottoms.

Such a statement is meaningless without specifying a cut-off. The definition of what constitutes a mountain and what represents a local hump varies with the resolution at which the surface is being viewed.

Humans do not interpret every grain of sand as a hill.

Skewness is a scale dependent property.
In 1D it vanishes at large length scales.

10. Stationary state skewness in 2D

Skewness is not tunable in $D > 1$.

The amount of skewness is a universal property of the KPZ stationary state height distribution (non-Gaussian).

Michael Lässig's operator product expansion closure conjecture requires stationary state skewness as well.

Chen-Chan Shin determined the amplitude ratio's

$$R_n = \frac{W_n}{(W_2)^{\frac{n}{2}}}$$

numerically for the RSOS and BCSOS models, and confirmed that their values are indeed universal.

11. Universal skewness amplitude ratio's in 2D

The amplitude ratio's $R_n = W_n/(W_2)^{\frac{n}{2}}$ converge smoothly to $R_3 = -0.27(1)$ and $R_4 = +3.15(2)$.

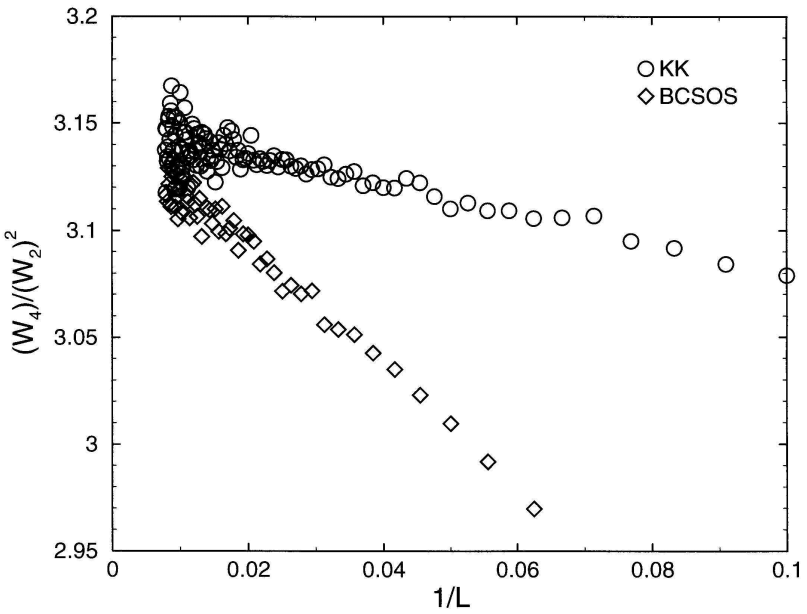

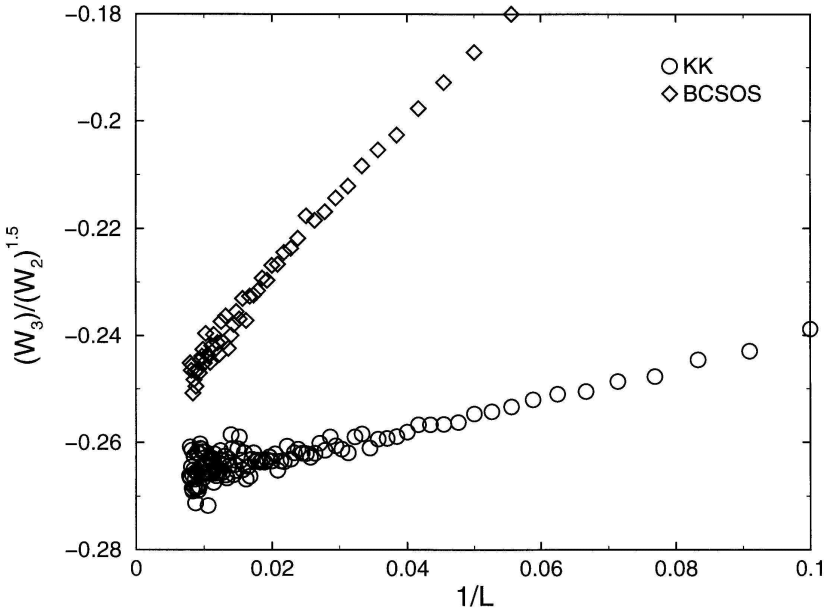

Skewness is negative, $R_3 < 0$.

Maybe $R_4 = \pi$. ($R_4 = 3$ in Gaussian distributions.)

12. Universal KPZ stationary state distribution function

KPZ growth is by probably the best understood system with driven non-equilibrium critical behaviour.

In 1D, the stationary state remains the trivial Gaussian distribution (uncorrelated up/down steps).

In 2D the stationary state is a novel non-Gaussian distribution, which needs still further investigation.

Lässig's conjecture is consistent with ALL current numerical data*.

(* Recently Parisi's group obtained more accurate MC data. They claim to see deviations from Lässig at the 1% level; but unfortunately their analysis is flawed).

C. RECONSTRUCTED ROUGH GROWING INTERFACES, RIDGELINE TRAPPING OF DOMAIN WALLS

Chen-Shan Chin and MdN, PRE 64, 031606 (2001)

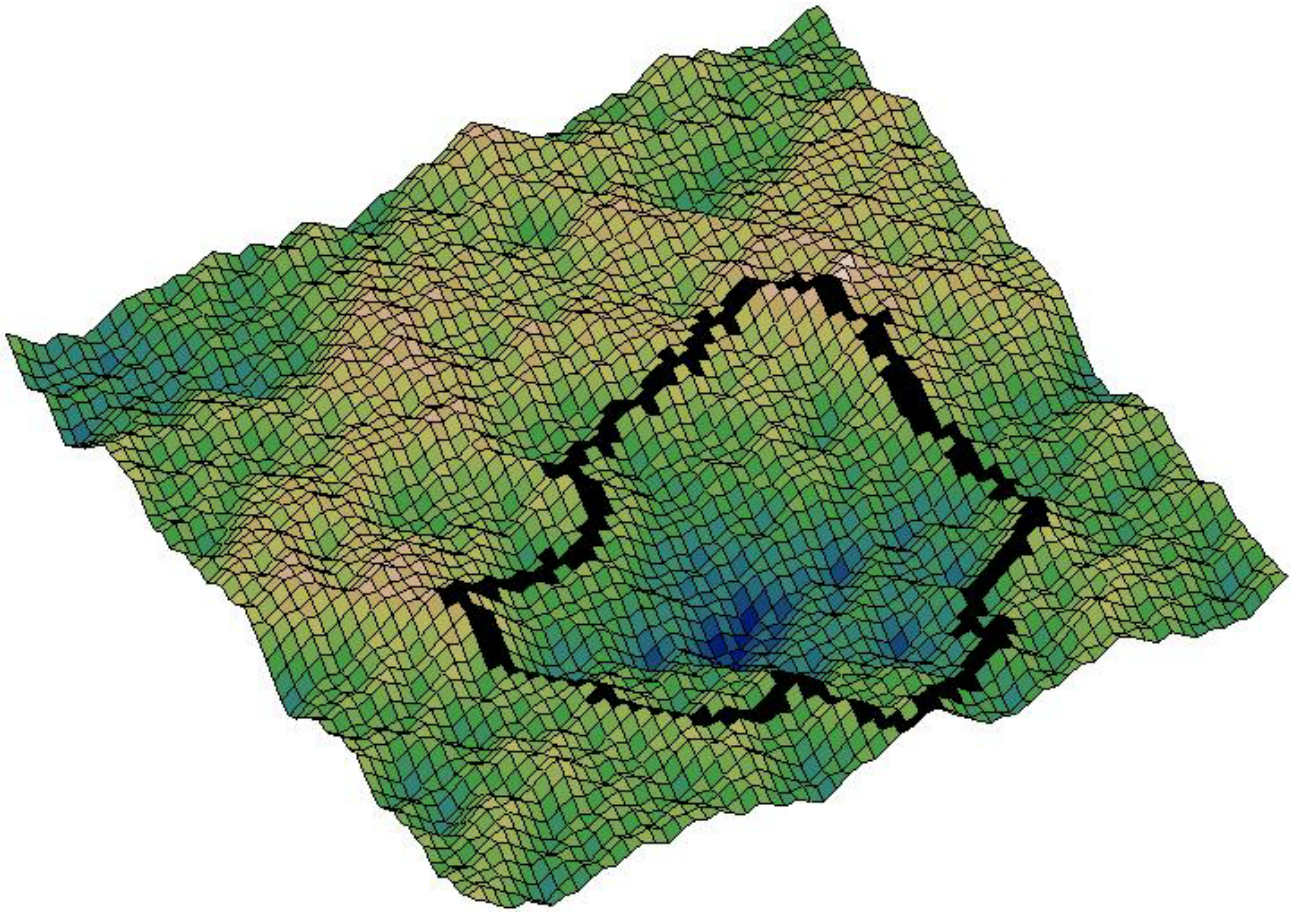

1. Surface reconstruction during growth

Question: Do surface reconstruction order-disorder phase transitions exist in stationary states of growing surfaces?

– Growing surfaces are always rough (although they might seem, e.g., to grow layer-by-layer at most experimental length scales for $T < T_R$).

– Reconstructed rough phases, and equilibrium deconstruction transitions exist while the surface is rough.

Question: Can reconstructed rough order exist in stationary states of growing surfaces like they do in equilibrium?

2. Missing row reconstruction in Au and Pt(110)

– Reconstructed rough order can not exist in MR FCC(110) facets.

– Steps excitations are topologically incompatible with the Ising type reconstruction order.

– Roughening induces a simultaneous deconstruction.

– Reconstructed rough order is topologically compatible with MR SC(110) facets.

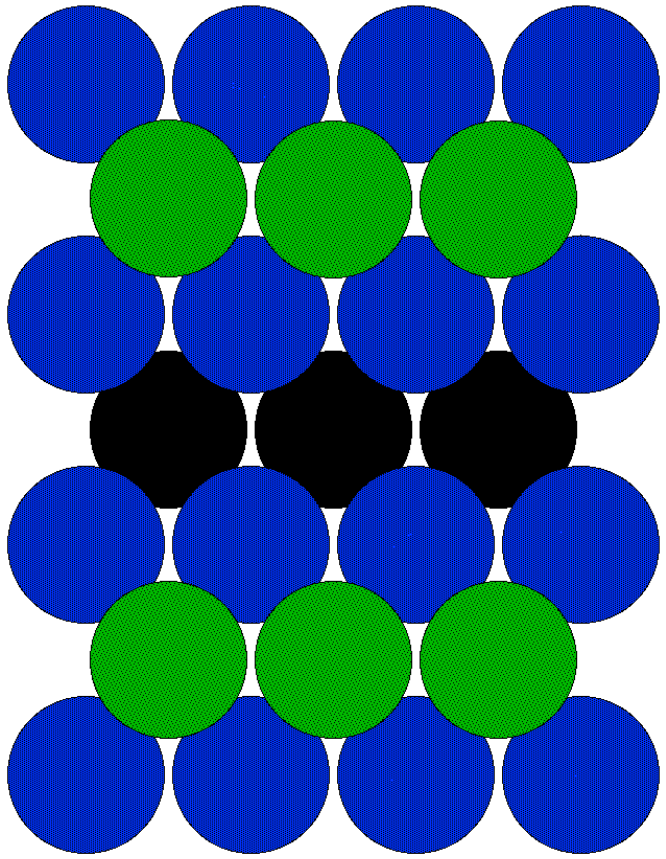

MdN PRB 46, 10386 (1992)

3. Reconstructed roughness in MR SC(110) facets

– Two distinct reconstruction order parameters:
* even or odd rows on top
* AF order in parity type
Ising spins: $S_r = \exp(i\pi h_r)$.

– Only 2 topologically distinct types of steps; each couples only to one order parameter type $\Rightarrow$ two types of RR order.

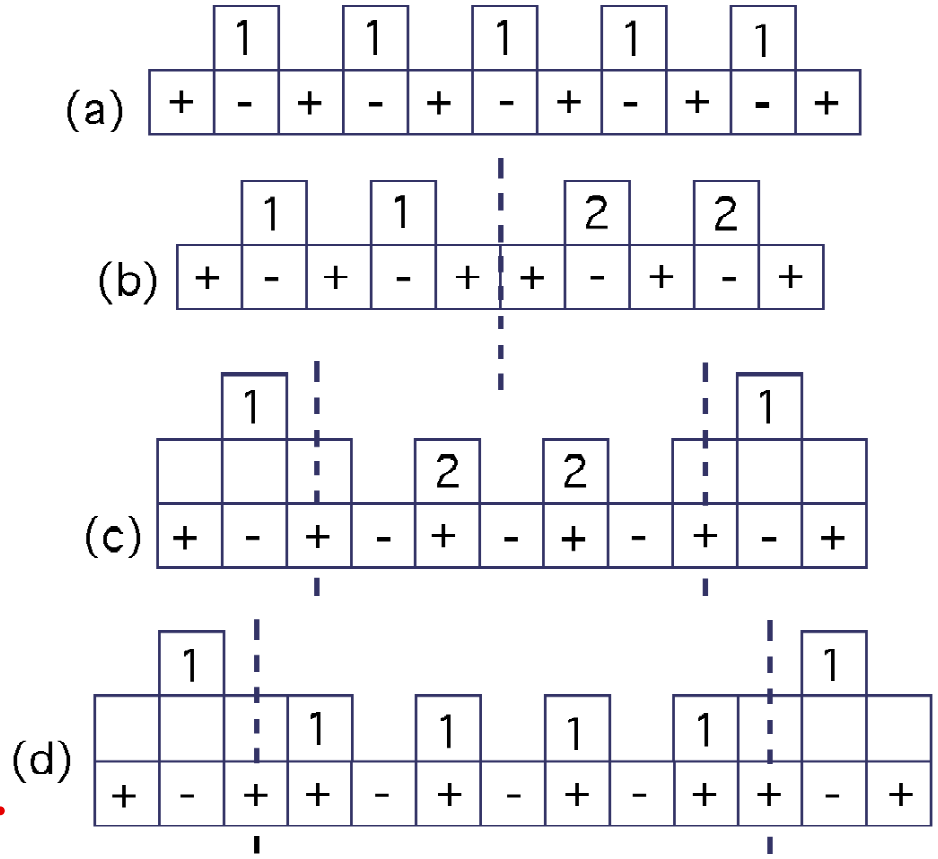

– step/wall energies, etc., determine whether the surface roughens before or after deconstruction, and which type of RR order can be realized.

4. 2D RSOS model with negative step energies

– nearest neighbours differ by $dh = 0, \pm 1$

– add nearest neighbour interactions

$E = \sum_{\langle i,j \rangle} K(h_i - h_j)^2$

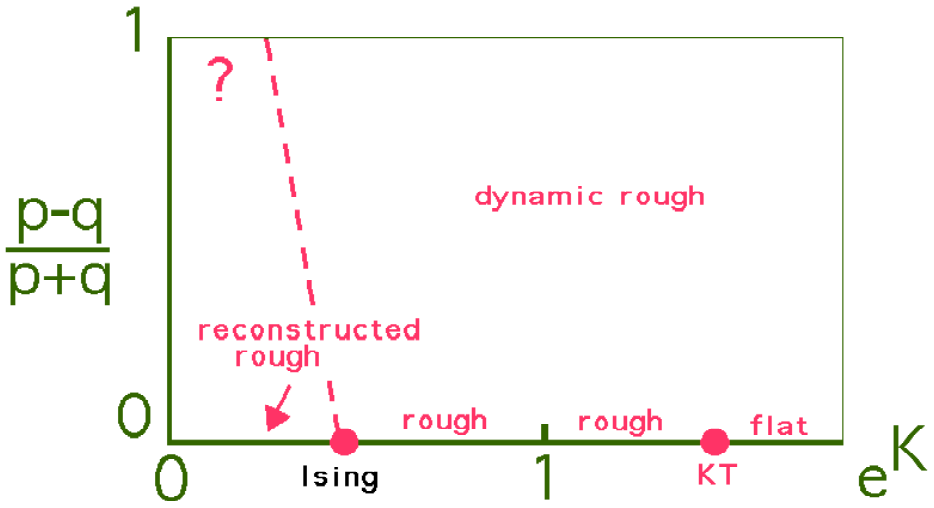

– In limit $K \to -\infty$ $dh = 0$ states frozen out (BCSOS model)

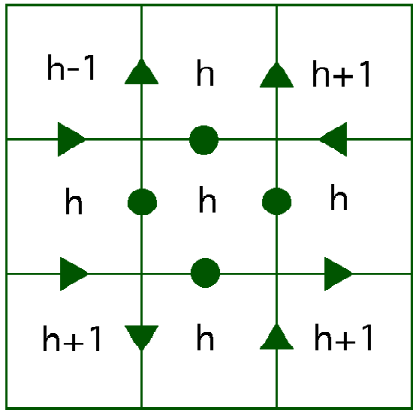

– checkerboard type RR order

– Ising type equilibrium deconstruction transition inside the rough phase (MdN 1985)

– A compact way to couple an Ising field to KPZ.

5. $K < 0$, RSOS Monte Carlo results: susceptibility

The RR checkerboard type order is characterized by $m = \langle (-1)^{x+y}\ S_r \rangle$ with $S_r = \exp(i\pi h_r) = \pm 1$.

The susceptibility peak, $\chi = L^2(\langle m^2 \rangle - \langle |m| \rangle^2)$ suggests a transition, but the peak scales with system size only as $\chi \sim L^2$ and keeps moving,

$$K_{\rm peak}(L) \simeq -A \ln(L/L_0)$$

$A = 0.77(5)$, $L_0 = 2.2(2)$

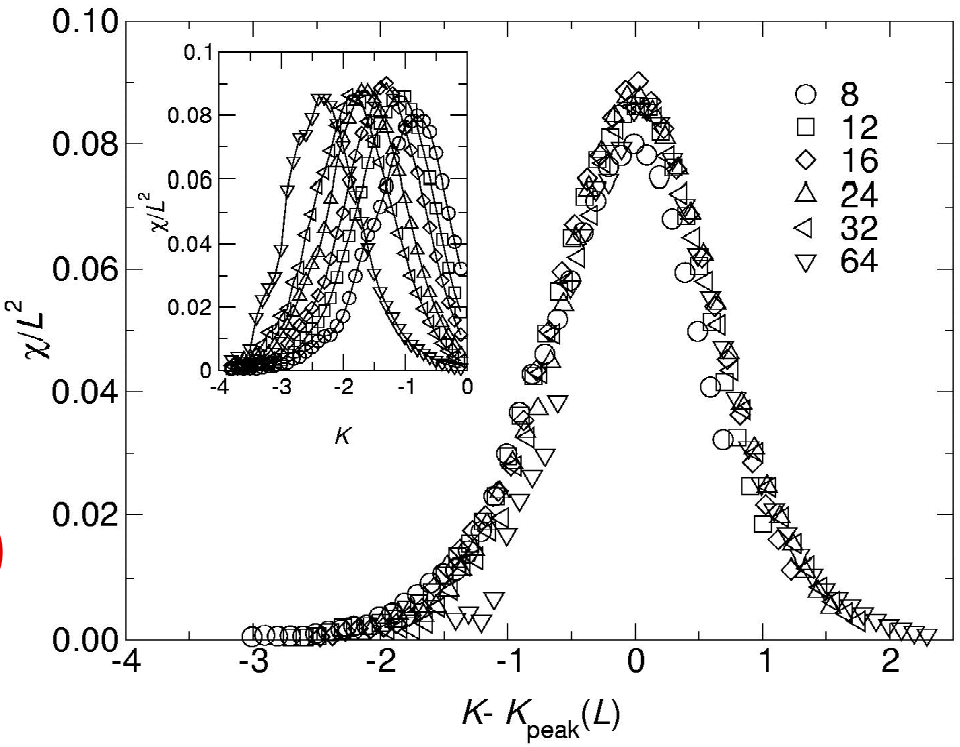

6. MC results: quasi-critical reconstruction fluctuations

Power law tails in the time series histogram of the staggered magnetization suggest critical fluctuations in the RR order for $K < K_{\mathrm{peak}}(L)$.

Quasi critical order exists within a length scale $l_{rec}(K)$ for every $K < 0$.

The susceptibility peak signals the K where $l_{rec}(K) \simeq L$.

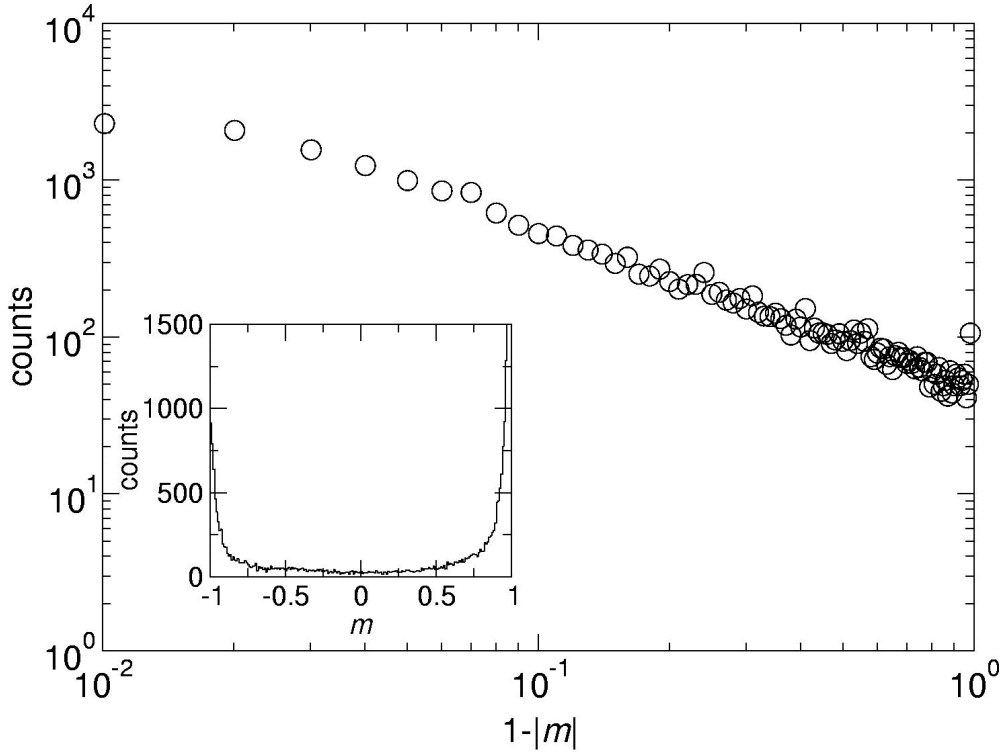

7. The life cycle of loops; ridge line trapping

– Reconstruction domain wall loops ($dh = 0$ contours) are nucleated in valley bottoms.

– Loops grow,subject to an up-hill bias until they coincide with a ridge line.

– A Loop remains strapped to the ridge lines until:

$\rightarrow$ another loop nucleation event annihilates it.

$\rightarrow$ KPZ fluctuations to which it is slaved fill-up the enclosed valley.

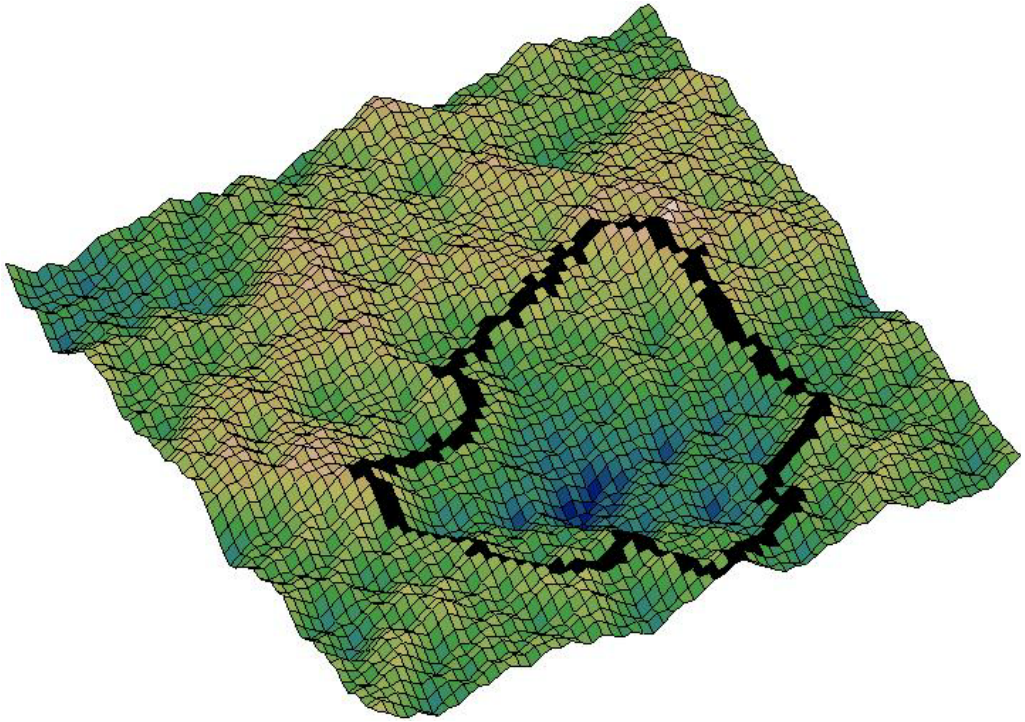

8. The nucleation of new loops

– Numerically:
$\tau_n \sim \exp(-aK)$ with $a = 3.0 \pm 0.1$
(in BCSOS time units).
Prepare surface in the BCSOS
KPZ stationary state at $K \ll K_c$;
record the intervals between
macroscopic loop events.

– Qualitatively:
Depositions remain indistinguishable
from KPZ growth events until $l_c^2 \simeq 6$
$\rightarrow \tau_n \sim L^{-2} e^{-4K}$.

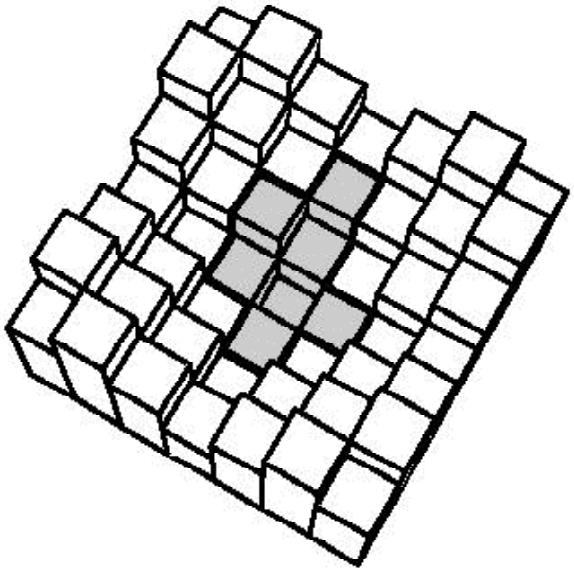

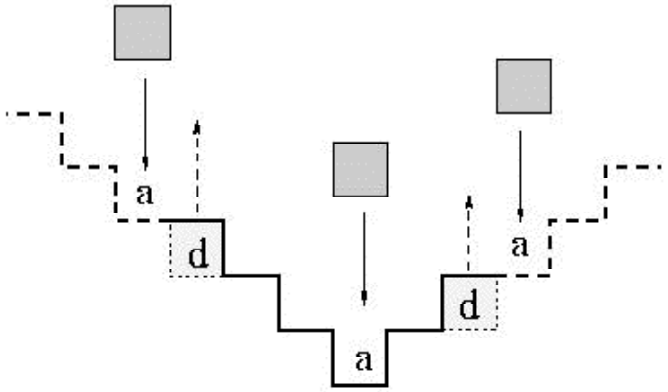

9. The KPZ trapping time scale

Measure the life time of a marked ridge line of diameter l on the KPZ growing surface.

The valley encompassed by the ridge line (it forms the watershed) vanishes by KPZ growth at a time scale $\tau_z \sim l^z$, with $z = \frac{8}{5}$.

The distribution of life times scales numerically with $z \simeq 1.7 \pm 0.1$.

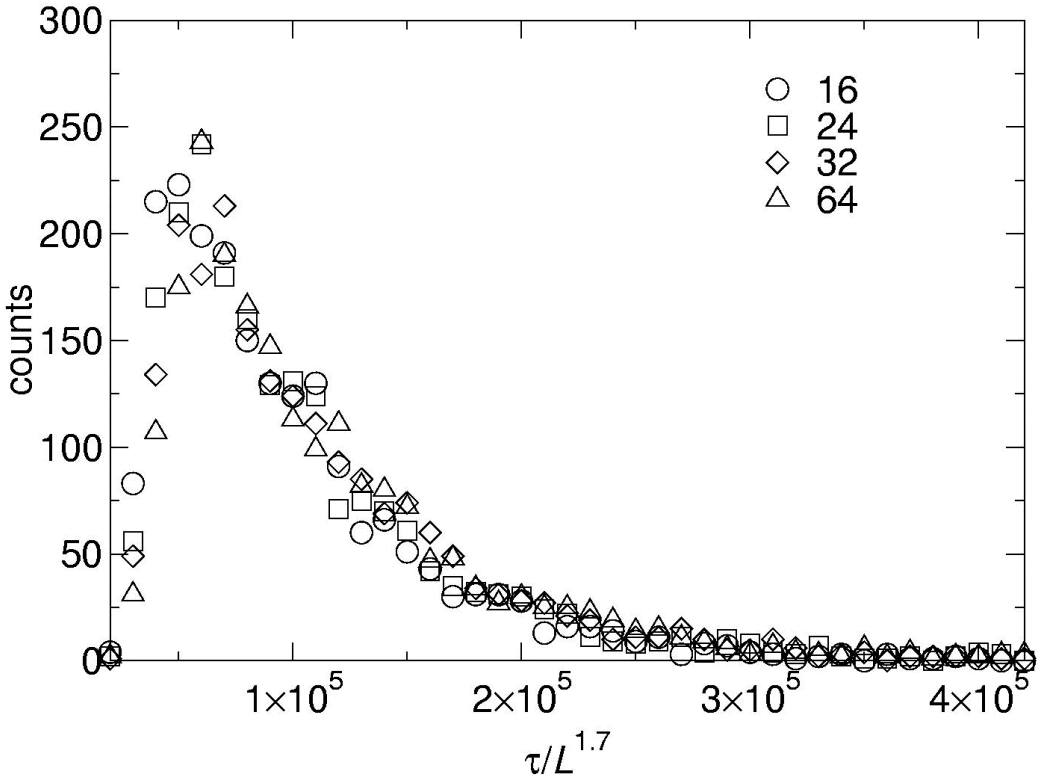

10. The crossover reconstruction length scale

KPZ critical fluctuations show up below a characteristic length scale $l_{\rm rec}$, where the nucleation time scale $\tau_{\rm n} \sim \exp(-aK)$ is larger than the KPZ time scale, $\tau_z \sim L^z$.

$$\tau_z \simeq \tau_n \quad \rightarrow \quad l_{rec} \sim \exp(\frac{a}{z}K)$$

The susceptibility peak shifts logarithmically, consistent with $\tau_n \simeq \tau_z \rightarrow K_{\rm c} = -\frac{z}{a}\ln(L/L_0)$.

(The amplitude of the shift is about 30% larger than z/α; we ignored, e.g., the self similarity of the rough surface and its ridge line network. Trapped loops can jump over adjacent subvalleys by nucleation events in those subvalleys. Such events renormalize the time scale τ_z.)

11. Conclusions

- During surface growth, the stationary states lack true macroscopic reconstructed rough order.
- Trapping of domain wall loops at ridge lines in the growing surface (caused by an upwards drift) is the fundamental mechanism.
- The competition between domain loop nucleation and ridge line KPZ fluctuations sets a temperature dependent crossover length scale $l_{rec}(K)$.
- Within l_{rec}, the surface appears as reconstructed rough, with quasi-critical fluctuations
(power law shape diffraction peaks) .

D. AN INTERFACE VIEW OF DIRECTED SANDPILE DYNAMICS

Chun-Chung Chen and MdN, PRE 65, March (2002), in press

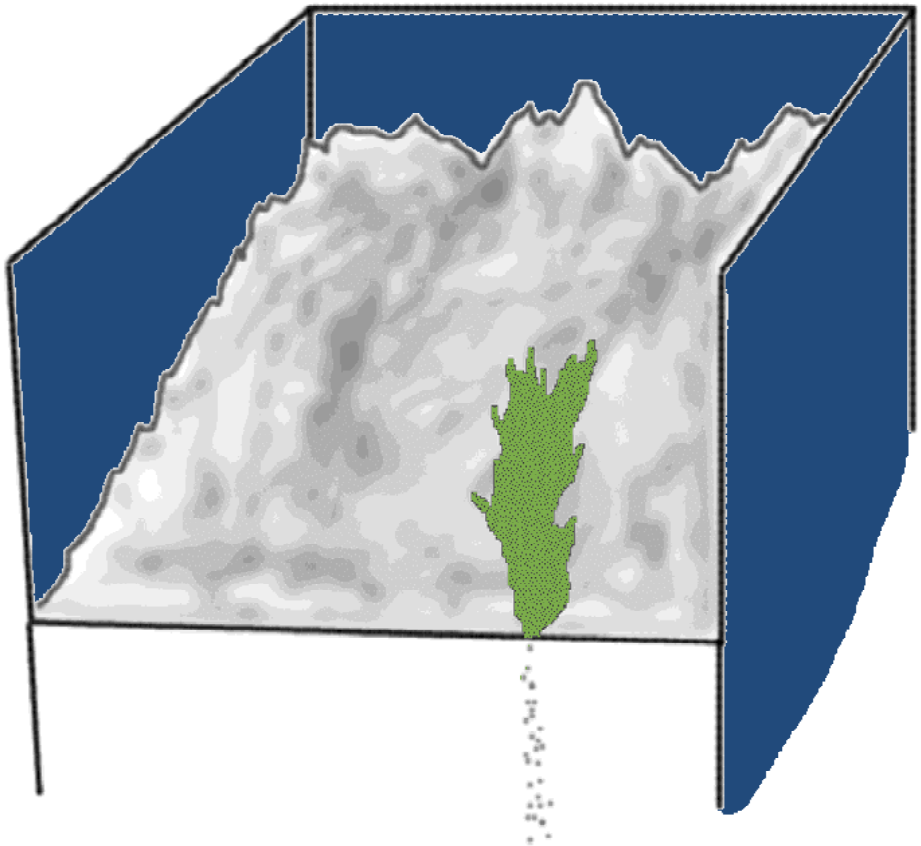

1. Avalanche dynamics versus surface growth

Avalanche phenomena are at the core of self organized criticality phenomena.

Our understanding of scaling properties of avalanches is still poor compared to, e.g., stochastic processes like surface growth and directed percolation.

Exact results are almost non existent.
The numerical convergence seems typically slow.

Efforts are underway to link avalanche processes to, e.g., directed percolation.

We construct a directed avalanche process that logically should belong to the KPZ universality class.

2. Unloading Sandbox

Imagine a box filled with granular material.

One of its four retaining walls is slowly lowered, such that the sand spills out from that side. This slowly unloads the box and establishes a sloped surface.

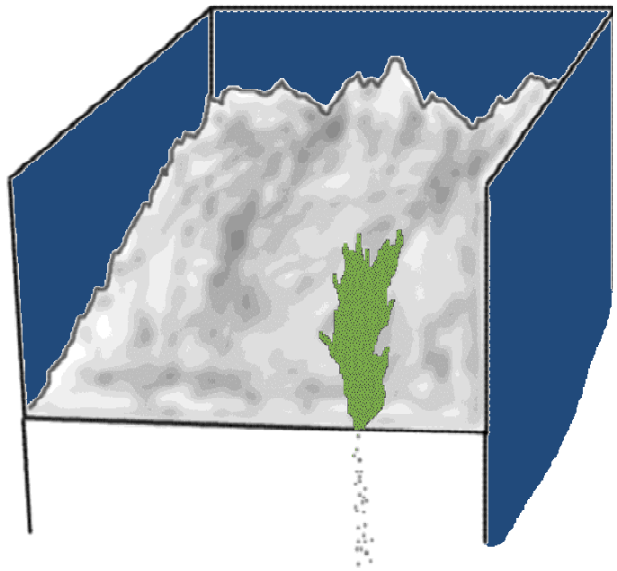

In the quasi static limit, the wall moves slowly enough that the unloading events are distinct avalanches.

Inspired by this we consider the following lattice model, with height variables $h(\mathbf{r})$ defined on a square lattice. They are either continuous or integer variables.

3. Stability condition

Avalanches propagate in the diagonal direction y.

Stability condition:

$$h(\mathbf{x},\mathbf{y}) \leq \min\left[h(x-1,y-1), h(x+1,y-1))\right] + s_c$$

Column $h = (x, y)$ is stable when the 2 heigths directly before it are both lower by more than a specific constant s_c.

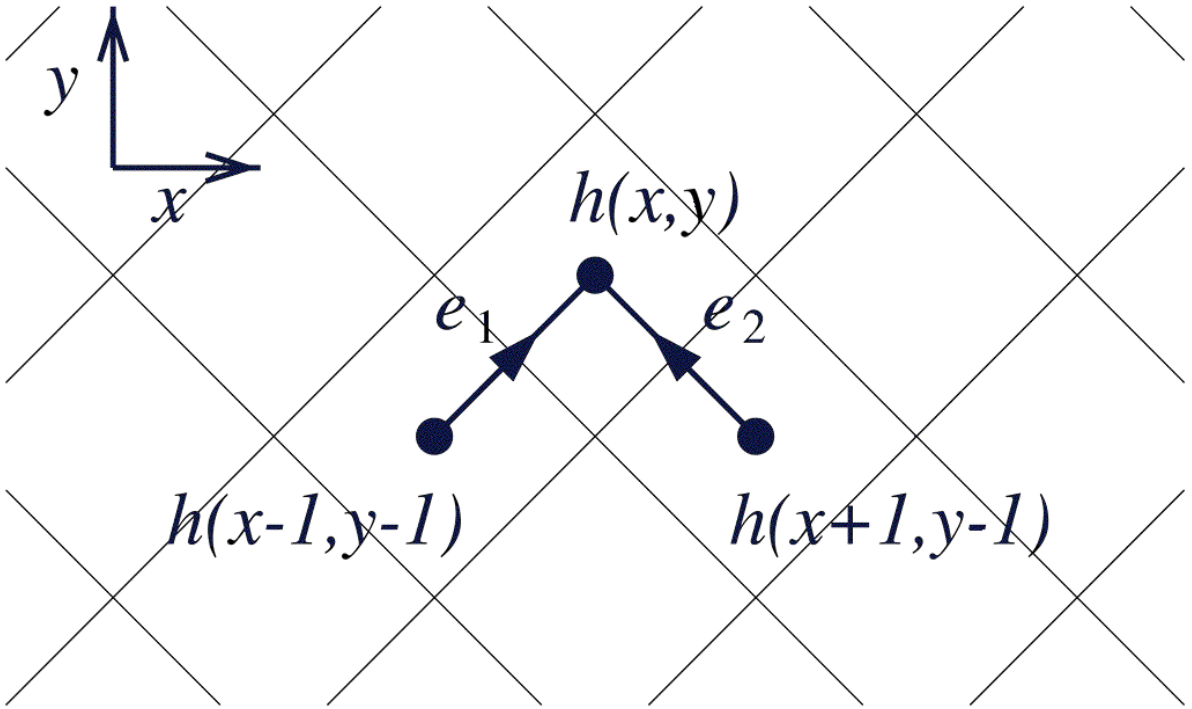

4. Toppling rule

Consider a stable configuration, after $n-1$ avalanches.

The n-th avalanche is triggered at the highest site at the $y=0$ driving edge, and reducing its height by a random amount $0 < \eta \leq s_c$.

This likely creates unstable sites in the $y=1$ row.
Those are updated as

$$h(x,y) \rightarrow \min\left[h(x-1,y-1), h(x+1,y-1))\right] + \eta$$

with η a random number between 0 and s_c.

Repeat this row-by-row until all sites are stable again.

5. 1D Surface growth connection

Every stable sloped surface configuration can be reinterpreted as the space-time configuration of a 1D growing KPZ surface due to the row-by-row Markovian nature of the stability and toppling rules.

In conventional KPZ dynamics MC runs are completely uncorrelated. This would amount to refreshing the entire sand box surface each “time”.

Instead, subsequent interface life-lines (MC runs) differ only inside the avalanche area.

From the interface growth perspective this represents a rather dangerous correlated type of MC run averaging.

6. The toppling rule belongs to 1D KPZ universality

Apply $h(x,t+1) = \min\left[h(x+1,t), h(x-1,t)\right] + \eta$ to the entire surface, row-by-row, to create a completely refreshed surface.

Step-1 (drawn $\rightarrow$ dashed): Equalize the $x \pm 1$ heights; choose the lowest of the two (always removes material) and call it $h(x)$.

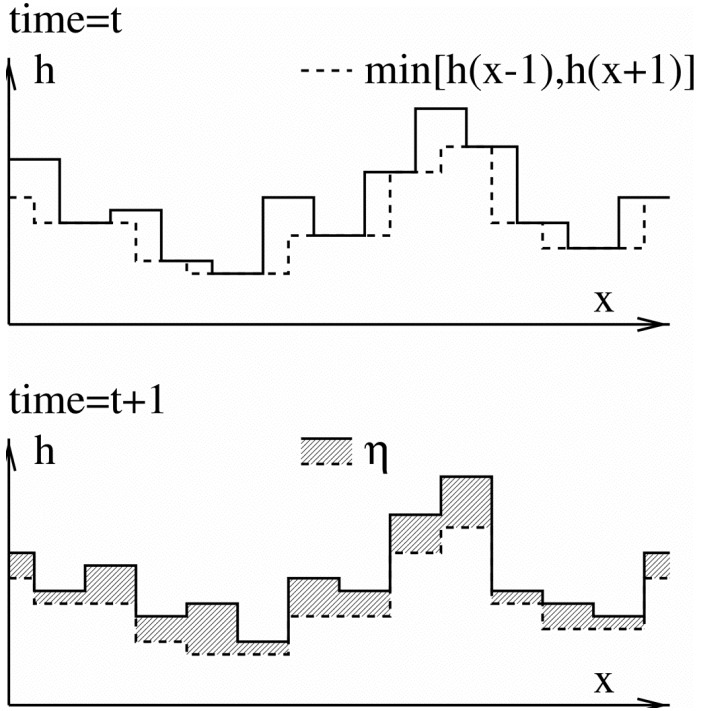

Step-2: All heights grow by a random amount η.

(x is only even (odd) at even (odd) times because of the diagonal lattice orientation.)

7. Numerical test of 1D KPZ universality

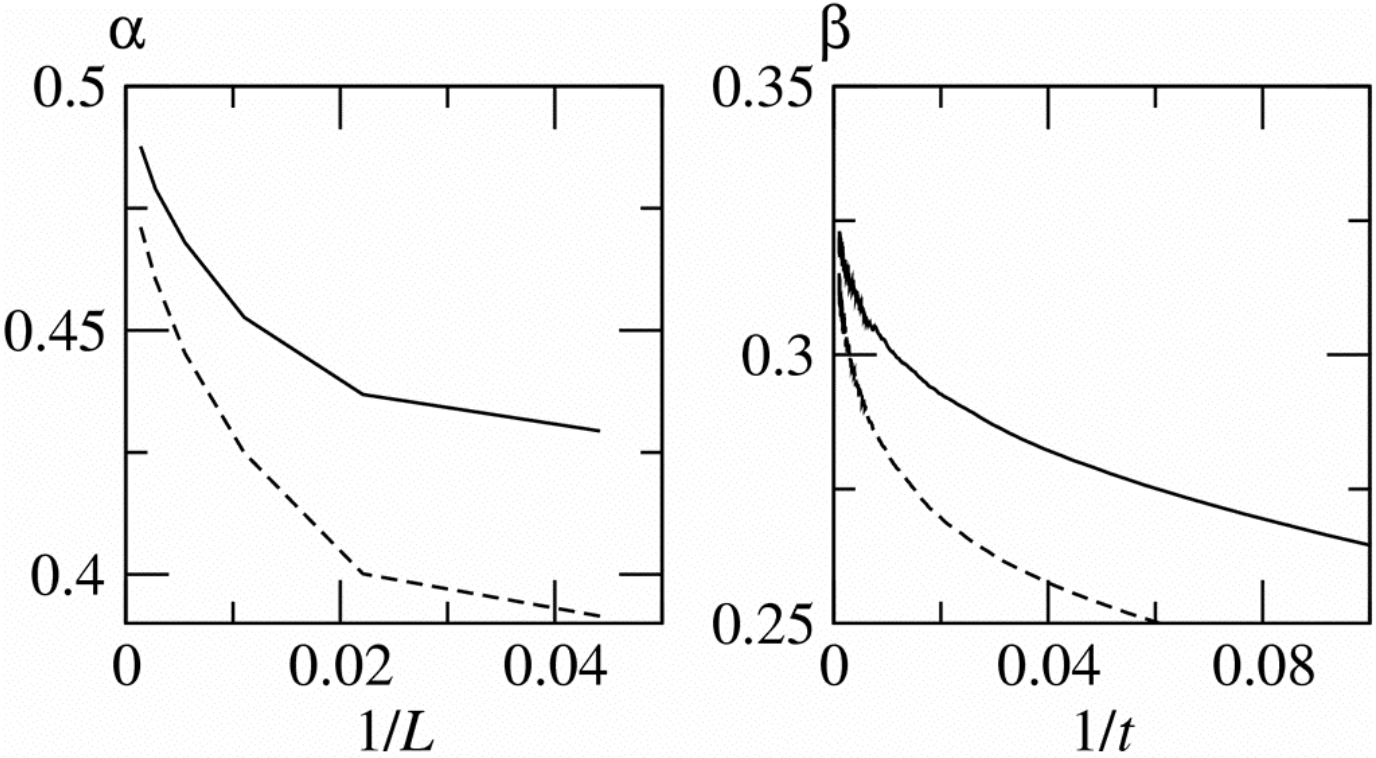

Scaling of the global surface width for an ensemble of completely refreshed surfaces: $W \sim L^{\alpha}$, and $W \sim t^{\beta}$ ($t \leftrightarrow y$). Agreement with 1D KPZ: $\alpha = \frac{1}{2}, \beta = \frac{\alpha}{z} = \frac{1}{3}$)

8. Avalanche distribution scaling exponents

The probability distribution for an avalanche with a specific characterstic width w, length l, and depth δ, is expected to obey the scaling form

$$P(l, w, \delta) = b^{-\sigma} P(b^{-z} l, b^{-1} w, b^{-\alpha} \delta)$$

Single parameter distributions, like $P_w \sim w^{-\tau_w}$, follow by integration over the other variables.

$$\tau_l = \frac{\sigma - 1 - \alpha}{z} \ , \ \tau_w = \sigma - z - \alpha \ , \ \tau_\delta = \frac{\sigma - 1 - z}{\alpha}$$

The mass of compact avalanches scales as $m \sim l \times w \times \delta$,

$$P_m \sim m^{-\tau_m} \text{ with } \tau_m = \frac{\sigma}{1 + z + \alpha}$$

9. Only 2 independent exponents if avalanches compact

Our dynamics does not conserve mass (it conserves slope). In the stationary state, the surface matches the lowering speed of the wall, such that the amount of removed sand per avalanche is on average equal to

$$\langle m \rangle = L_y \times \frac{1}{2} s_c \;\rightarrow\; \sigma = 2 + z + 2\alpha.$$

These exponent identities are valid beyond our KPZ type unloading sandbox. They apply also to, e.g., the EW type avalanche models by Paczuski $et\ al$ and Kloster $et\ al$, and to the random walker type exactly soluble directed avalanche model of Dhar and Ramaswamy.

10. Numerical results for the avalanche exponents

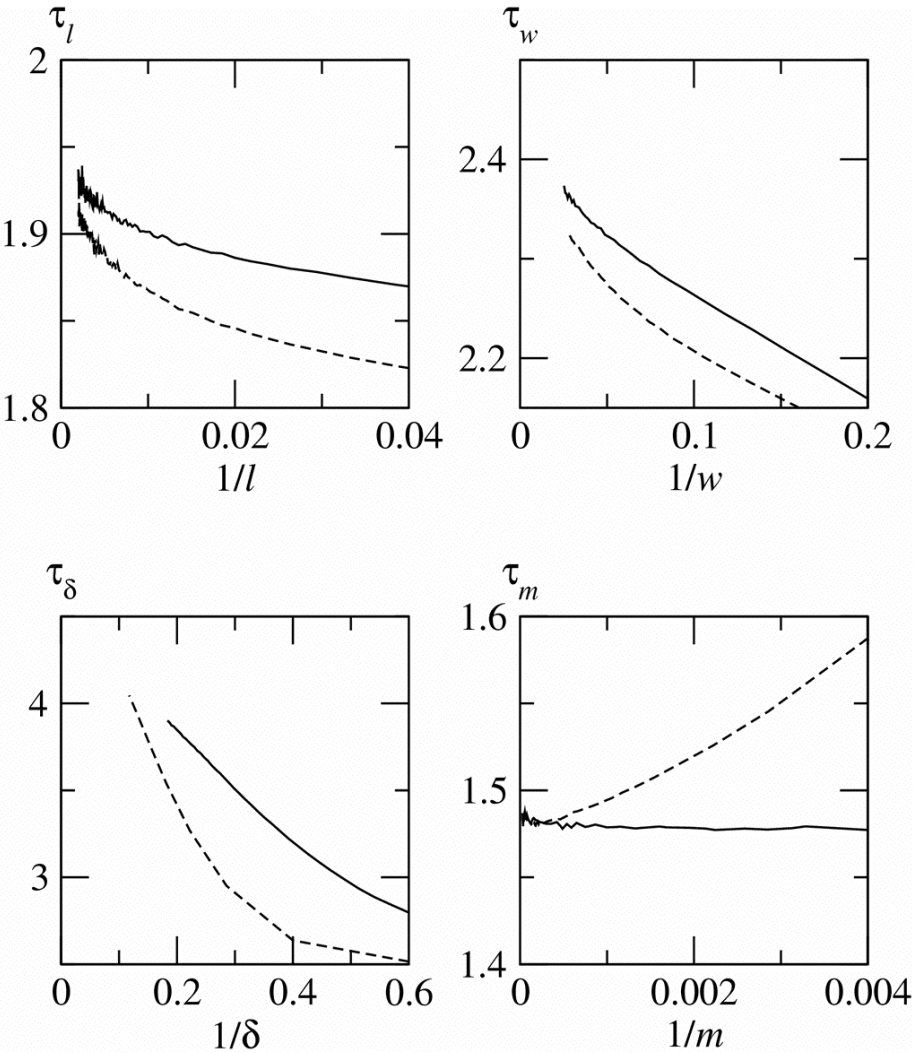

(2^{31} avalanches)

MC simulations for the discrete (dashed) and the continuous heights (drawn) sandbox model.

KPZ scaling predicts
$\alpha = \frac{1}{2}, z = \frac{3}{2},$
Compactness implies
$\sigma = \frac{9}{2}$

$$\Rightarrow \begin{array}{l} \tau_l = 2, \tau_w = 2.5 \\ \tau_\delta = 5, \tau_m = 1.5 \end{array}$$

11. Numerical results for the avalanche exponents

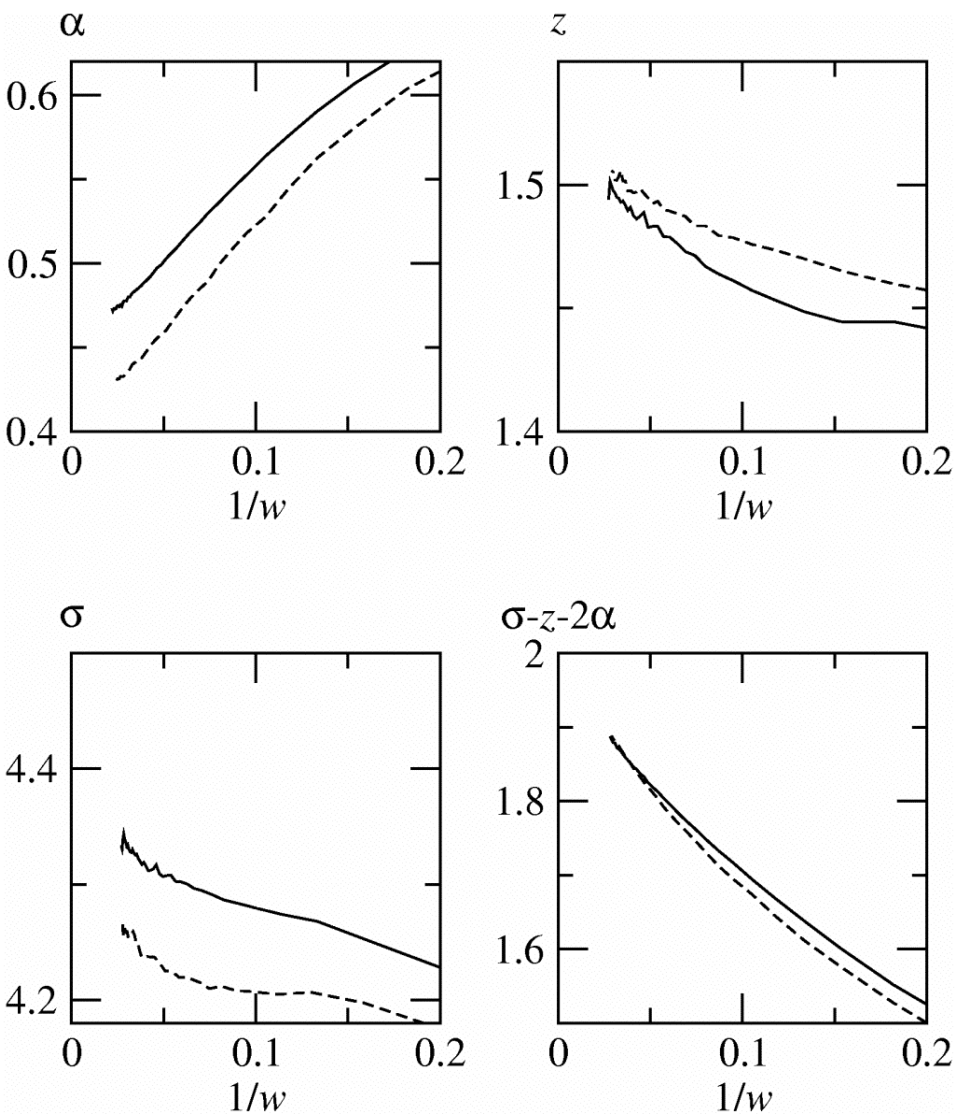

The same MC data in terms of:

$\alpha = 0.46 \pm 0.01,$

$z = 1.52 \pm 0.02,$

$\sigma = 4.43 \pm 0.05$

The compactness exponent relation

$2 = \sigma - z - 2\alpha$

is well satisfied.

The convergence to

$\alpha = \frac{1}{2}$ and $z = \frac{3}{2}$

is shaky.

12. Correlated Monte Carlo sampling

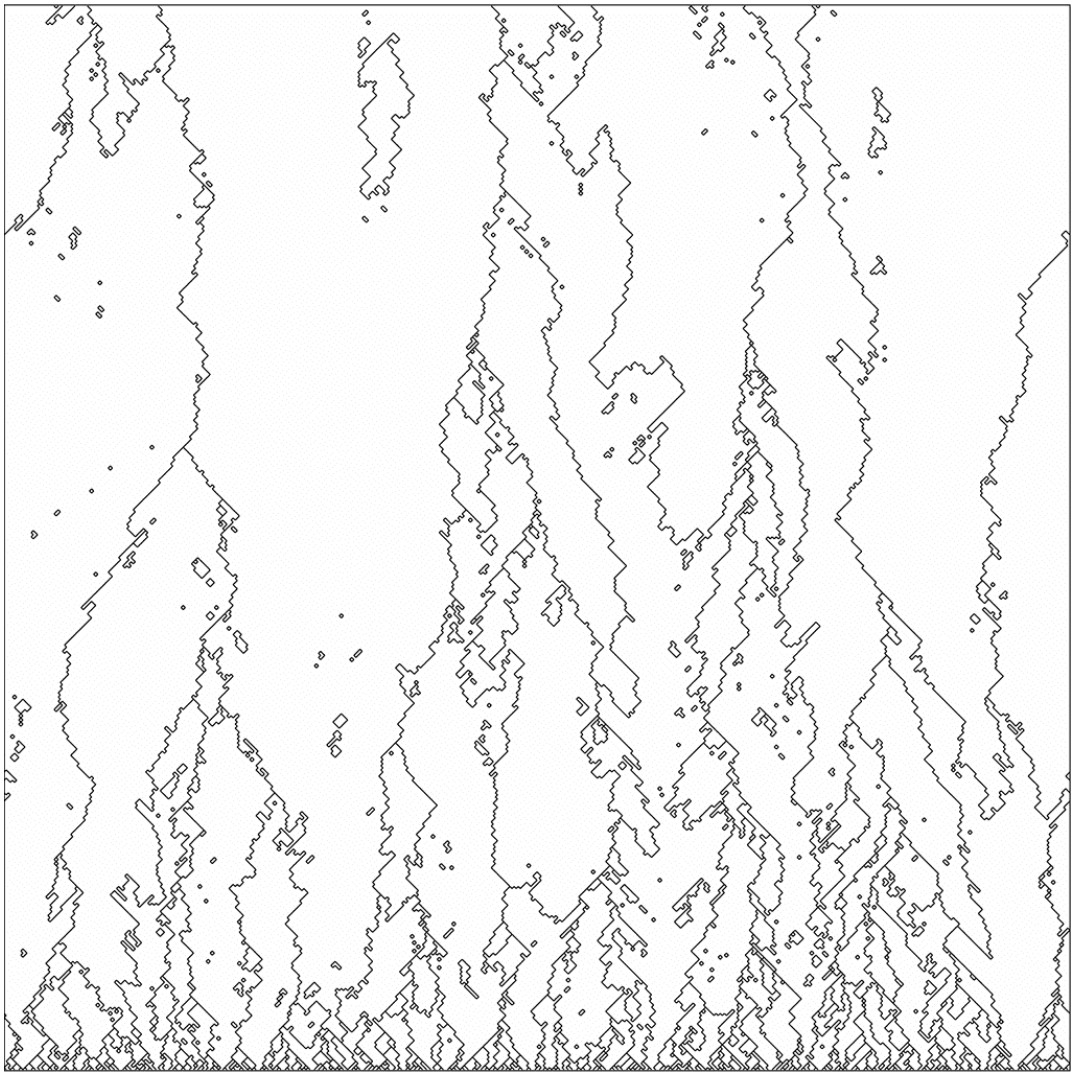

The surface ages in a correlated way from scars left by previous avalanches (their edges).

In KPZ language the MC runs are correlated.

Does this affect the interface width?

13. First avalanche statistics

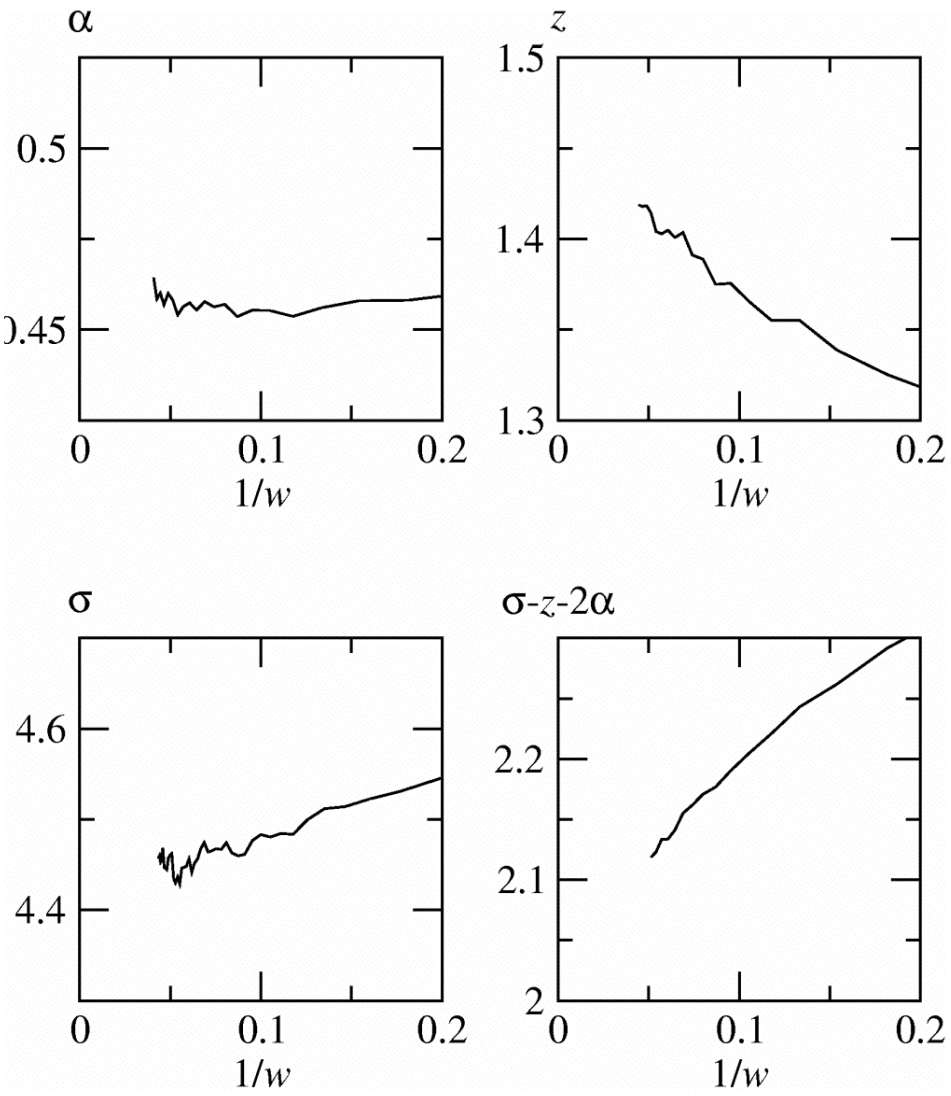

Test -1:
Take out the aging.

Distributions for the first avalanche on a fresh sand surface.

$z \rightarrow \frac{3}{2}$ smoothly

α does not cross $\frac{1}{2}$ anymore. α still too small (short avalanches in the ensemble enhance the FSS effects !?)

14. KPZ width for avalanche correlated MC runs

Test 2: Global KPZ interface width using avalanche correlated Monte Carlo sampling (drawn lines) versus uncorrelated sampling (dashed lines).

The scaring/aging enhances the surface roughness at intermediate times (the bumps).

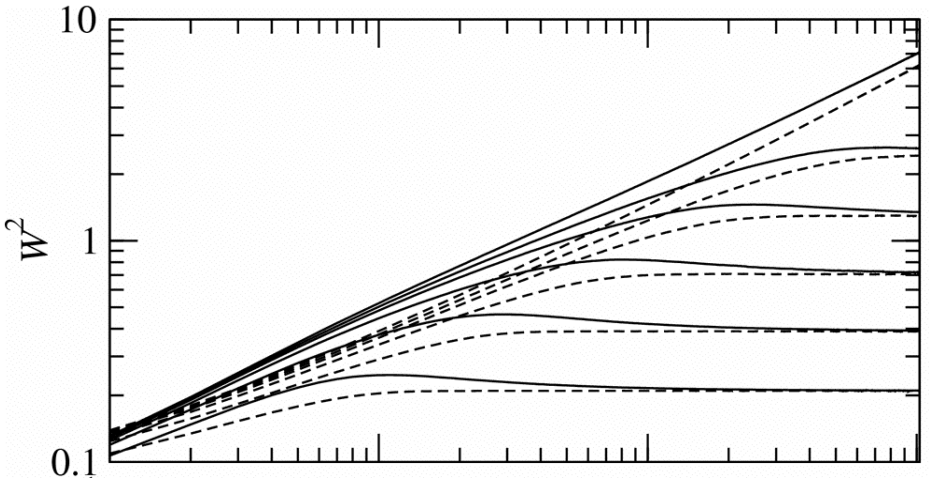

For $t > L_x^z$: same width as for uncorrelated sampling. Large avalanches span the entire system in the x direction and refresh the entire surface at large t periodically.

15. Surface width scaling for correlated MC runs

Most avalanches are limited to the scarred part of the surface. For their scaling properties we should define a roughness exponent α^* based on the scaling of the diverging maxima of $W(t)$ with L_x.

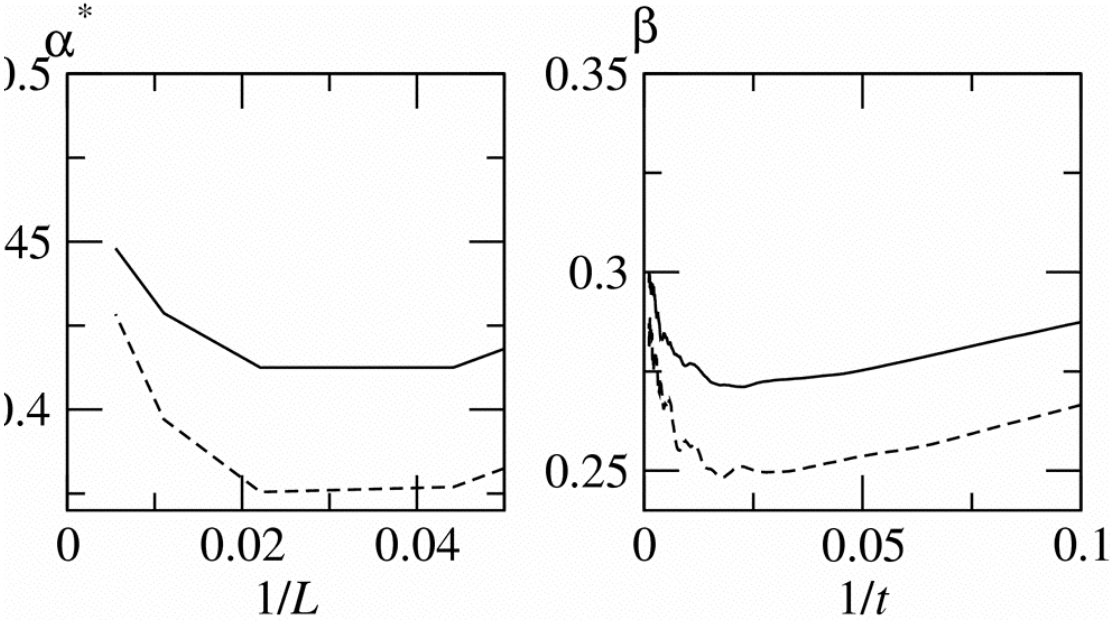

$W \sim t^\beta$ is sensitive to the bumps in $W(t)$ as well.

Do these α^* and β, converge to the KPZ values ($\frac{1}{2}$ and $\frac{1}{3}$)?

16. <u>It is only a crossover scaling effect!</u>

The difference between the squared widths of avalanche correlated MC runs and completely uncorrelated MC runs, $\Delta W^2 \sim t^s$ scales with exponent $s \simeq 1/3$.

The maxima in the width curves are a transient finite size scaling effect, since the total width scales as $W^2 \sim t^{2/3}$.

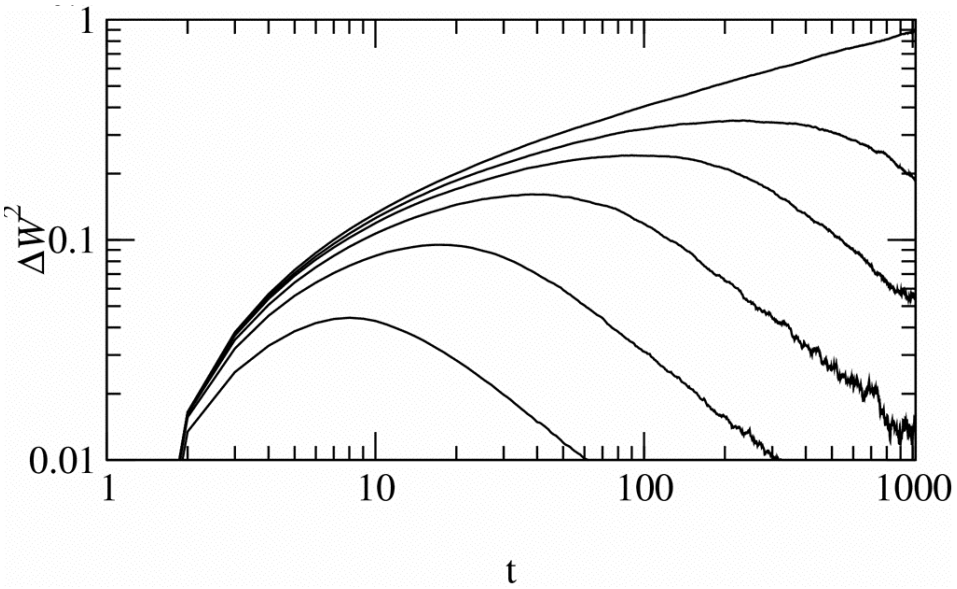

$\Rightarrow$ The KPZ exponents for avalanche correlated and uncorrelated MC runs are asymptotically the same.

But with very severe and slow crossover scaling !!!

17. The crossover represented as a scaling field

Presume that the corrections to scaling caused by the avalanche correlations can be mimicked by adding a local interaction $uO_{sc}(x)$ to the KPZ equation.

$$W^2(t,u_{sc}) = t^{\frac{2\alpha}{z}} S(t^{\frac{y}{z}} u_{sc}) = t^{\frac{2\alpha}{z}} \left[A + t^{\frac{y}{z}} u_{sc} B + \cdot\cdot \right]$$

The scaling index of this irrelevant scaling field must take the value $y_{sc} = -\alpha$ to account for $\delta W^2 \sim t^{1/3}$. Moreover the operator must scale as

$$O_{sc}(x) \sim b^{-x_{sc}} \text{ with critical dimension } x_{sc} = z,$$

according to power counting (that $u_{sc}\, O_{sc}$ and $\partial h/\partial t$ in the KPZ equation scale alike).

18. Rounding of the sand surface near the driving edge

The same crossover operator is responsible for enhanced rounding of the surface slope $s(y)$ near the driving edge:

$$\Delta s(y) = s(y) - s_0(y) \sim y^{\kappa}$$

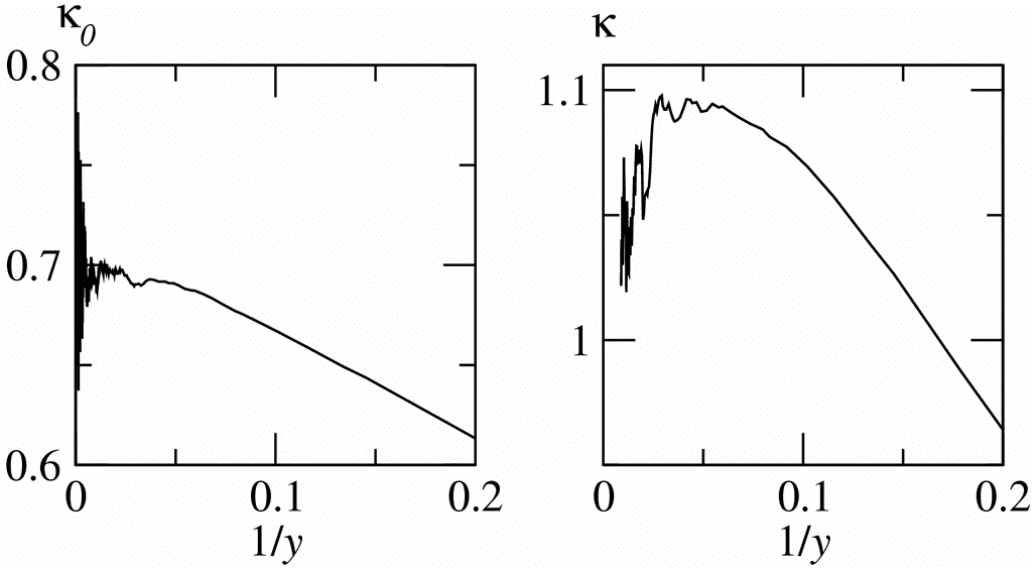

For uncorrelated MC runs the slope is already rounded as $s_0(y) = s_\infty + Ay^{-\kappa_0}$ with $\kappa_0 \simeq \frac{2}{3}$.

Our numerical value $\kappa = 1.05 \pm 0.07$ is in agreement with $\kappa = x_{sc}/z$ implied by mystery operator O_{sc} with scaling dimension $x_c = z$.

19. Identifying the crossover scaling operator

We identify O_{sc} from an analytic self-consistent type derivation for $\Delta s(y)$ that reproduces correctly $\kappa = 1$.

O_{sc} is proportional to the density of scar lines and the angles they make with respect to the y-axis. It's sign depends on whether the scar was a right or left boundary of the avalanche that created it.

$$O_{sc}(x,t) \sim \frac{\hat{e}_y \cdot \nabla g}{|\nabla g|}$$

$g(x,t)$ is an age-field representing how many MC time steps ago site (x,t) was updated. The denominator arises because the magnitude of the age jump across the scar line, $|\nabla g|$, does not play a role.

20. Conclusions

We construct a 2D directed avalanche model that belongs to the 1D KPZ universality class.

Each stable 2D sand surface represents a world sheet of the 1+1 dimensional growing interface.

The avalanche distributions for length, width, depth, and mass, follow KPZ scaling, but · · · · · · the corrections to scaling are large and slow, and can fool you.

From the KPZ perspective this is caused by correlated MC sampling; MC runs differ by only one avalanche.

Our model sheds light on generic difficulties in generating high quality numerical results for SOC dynamics.